FIELD THEORY OF FRUSTRATED ANTIFERROMAGNETS : AN APPROACH TO THE KAGOME LATTICE MODEL

by

D.SHUBASHREE

A THESIS IN PHYSICS

Presented to the University of Madras in Partial Fulfillment of the Requirements for the Degree of Doctor of Philosophy

November 1997

The Institute of Mathematical Sciences
C.I.T. Campus, Taramani,
Madras 600113 INDIA

CERTIFICATE

This is to certify that the Ph.D. thesis titled *Field Theory of Frustrated Antiferromagnets : an approach to the Kagome Lattice Model* submitted by *D.Shubashree* is a record of bonafide research work done under my supervision. The research work presented in this thesis has not formed the basis for the award to the candidate of any Degree, Diploma, Associateship, Fellowship or other similar titles. It is further certified that the thesis represents independent work by the candidate and collaboration was necessitated by the nature and scope of the problems dealt with.

R. Shankar

November 1997

Thesis Supervisor

ACKNOWLEDGEMENTS

My thanks to Prof R.Ramachandran, the Director of Matscience for having given me the opportunity to work here.

My deep gratitude to my advisor Dr. R. Shankar, who has helped me learn much during my stay here and thanks to Drs G.Rajasekaran, M.V.N. Murthy, T.R.Govindarajan, T.Jayaraman, Madan, Radha Balakrishnan.

It has been a lovely opportunity to interact with Mary, Pari, Ravindran, Swarup, Manisha, Vinod, Prakash, Kamal, Jam, Deepak, Nandini,Jayajit, Sarasij,Suneetha, Manoj, Radhika, Madhu, Tabish, Enakshi Bhattacharya, Lakshmi Govindarajan, Preethi, Deepthi and for a short spell Sudeshna Sinha, Neelima Gupte,and Shreesh.

The support and encouragement offered to me by my parents, grand parents, Raja, Kala is something without which of course nothing could have been achieved.

Nothing could have been achieved, without the support of all the administrative staff. the faculty and members of the institute of Mathematical Sciences and many others whom I may forget to mention at this juncture.

Contents

Chapter 1

Introduction

Low lattice dimensionality and frustration are known to produce interesting effects in quantum antiferromagnets. Some important consequences of these features in magnetic systems are ground states exhibiting novel order. This aspect of frustrated Heisenberg antiferromagnets has been the motivating factor of much work done in the field. In this thesis we study the ground states and low lying excited states of some models exhibiting these features.

In the 1-D spin chain, due to low dimensionality, fluctuations destroy the Neel order and the ground state is a spin singlet. In two dimensions there is a strong tendency of fluctuations to drive the system to disorder. This can be seen also in the nearest neighbour Heisenberg antiferromagnet on a square lattice. Even for S $= \frac{1}{2}$, the ground state possesses long range Neel order. However as seen, for instance, in spin wave theory [1], the ordered moment is reduced by about 40 % indicating the tendency of the strong quantum fluctuations to drive the system into a disordered phase. The $SO(3)$ spin symmetry is broken down to a symmetry of rotation about the axis picked out by the order parameter which is the staggered magnetization vector. The low

lying excitations about this state are the two branches of gapless goldstone modes with a linear dispersion. They indicate the breaking of the $SO(3)$ spin symmetry to an $SO(2)$ symmetry of rotations about the axis picked out by the magnetization vector.

Frustration alters this picture drastically, an example of which can be seen in the case of the nearest neighbour Heisenberg antiferromagnet on the triangular lattice (TLAF). The ground state spin configuration of the classical model is no longer the collinear Neel state but is deformed into the 120 ° planar spiral. The spin rotational symmetry is completely broken in this case and the lowest lying excitations are the three branches of gapless spin wave modes. The stiffnesses governing these excitations are different as indicated by the spin wave velocities being different for the in plane and out of plane fluctuations [2].

Naively, the inclusion of quantum effects can be expected to push this either way. On the one hand fluctuations can act in order to relieve the frustration and impose an order, or when very strong they can greatly reduce or even destroy the classical order thereby favouring a state with no long range spin order. In this picture, the effect of a large co-ordination number is generally expected to suppress the effects of fluctuations. We look at the TLAF, which has been studied widely in some now look at some aspects of the TLAF. This system has been widely studied and is well understood and serves as a good reference point for a comparitive analysis.

1.1 The Triangular lattice antiferromagnet.

The TLAF has been analysed in depth by semiclassical approaches, numerical and exact diagonalization studies etc. One obvious choice for a good ordered ground state of this model is the 3 sublattice 120° helical state also referred to as the $\sqrt{3} \times \sqrt{3}$ state. This is the type of order present in the ground state of the classical TLAF. Among disordered states, the resonating valence bond state[3], made up of resonating superpositions of pairwise singlet combinations of the spins is one choice.

Of these, by now there is plenty of evidence from different approaches that the $\sqrt{3} \times \sqrt{3}$ state is the preferred choice. For instance, a variational estimate of the upper bound to the ground state energy of the TLAF is found to be $E_{gs} \leq -.1789$ J/bond [4] by Huse et al. They also show that the resonating valence bond state exceeds this bound by a large amount. Following up on this with a conventional spin wave analysis, Jolicoeur et al [2] conclude that the $\sqrt{3} \times \sqrt{3}$ state which has $E_{gs} = -.1769$ J/bond is a good approximation to the actual ground state. They also show that $< S_z >= 0.239$ for $S = \frac{1}{2}$ which constitutes a 60% reduction in the sublattice magnetization. The lowest lying excitations about this state are three branches of gapless spin wave modes. The spin wave stiffnesses for these excitations are different for the in plane and out of plane fluctuations as indicated by the corresponding spin wave velocities. This survival of $\sqrt{3} \times \sqrt{3}$ long range order is reinstated by the high temperature series expansion of Elstner and Young [5] and by Bernu et al [6] who also arrive at this conclusion based on a computation of the exact

spectra of periodic samples.

Field theoretic techniques used in unfrustrated antiferromagnets is, such as the nearest neighbour antiferromagnets on the square lattice can be extended to frustrated models [7, 8] In the case of the TLAF the order parameter is an element of the group SO(3) and the corresponding field theory is the $SO(3)_R \times SO(2)_L$ non-linear σ model[9, 10, 11]. In this model the $SO(3)_R$ symmetry group is the original spin rotational symmetry. The $SO(2)_L$ is a symmetry of the low energy modes only and it is not present in the microscopic model.

For the TLAF the parameters of this theory have been derived starting from the microscopic lattice model in [9]. A renormalization group analysis of a model having the above symmetries [10] shows that there are 2 regimes in parameter space, a strong coupling regime indicating a quantum disordered phase with no long range spin order and a weak coupling regime with long range order where the coupling constants and correlation functions are merely renormalized from their classical values by quantum fluctuations. This is parallel to the spin-wave theory which predicts long range helical spin order with a reduced moment even for the case of S=$\frac{1}{2}$ where the quantum effects are most pronounced.

The consensus from various approaches is that the ground state of the TLAF, has $\sqrt{3} \times \sqrt{3}$ long range order, with an order parameter in SO(3) and three gapless low lying modes corresponding to the complete breaking down of the spin symmetry.

A much more complex picture is given by the Kagome lattice antiferro-

magnetic model (KLAF). This is a system with a geometry very similar to the TLAF but with a lower co-ordination number of 4. Before defining the various problems associated with this model, we describe earlier known results.

1.2 The Kagome lattice antiferromagnetic model.

The Kagome lattice which is shown in figure 1.1 has a geometry very similar to the triangular lattice in the sense that it can be superposed exactly on a triangular lattice of the same dimensions. It contains only $\frac{3}{4}$ the number of points as the triangular parent. Further there are several new features in the

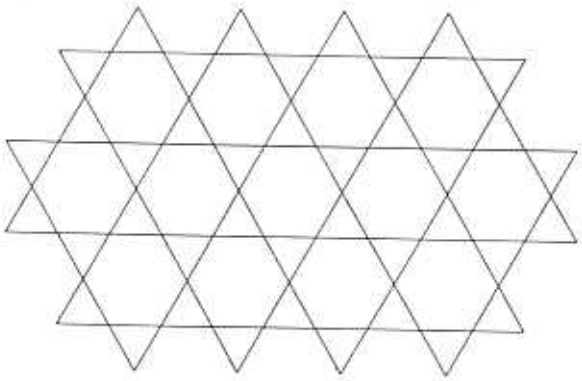

Figure 1.1: The Kagome Lattice

KLAF compared to the TLAF some of which are described here. For instance the huge degeneracy in the ground states of the classical model [12, 13], is a major difference. This degeneracy arises as follows.

1.2.1 Ground states of the classical KLAF

The nearest neighbour Heisenberg model is defined by the hamiltonian

$$H = \sum_{<i,j>} \vec{S}_i.\vec{S}_j \tag{1.1}$$

where, $< i, j >$ implies that the sum is over all j that form nearest neighbours to i. One of the first things that we notice about the KLAF is the huge ground

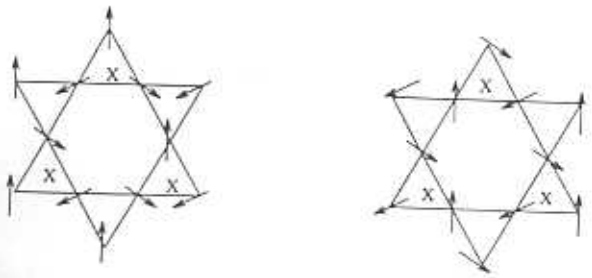

Figure 1.2: Small sections of the KL showing examples of coplanar (potts) ground state configurations superposed on it.

state degeneracy[13]. Referring to figure 1.1 and equation for the Hamiltonian (1.1) we notice that the energy described by (1.1) is minimised by any spin configuration for which the sum of the spins on an elementary triangular plaquette is zero. We also immediately notice that this leaves a huge degeneracy, even apart from global spin rotations and other symmetry operations, which stems from the different ways of fitting these units together. The different coplanar states which are obtained by permutations of the three spin orientations can be mapped on to the representations of the three state Potts model.

Some of the coplanar configurations all of which satisfy the above condition but show, locally, very different structures are shown in figures 1.2 and 1.4. Besides these there are also non-coplanar configurations which with reference to figure 1.3 can be generated from some of the planar configurations by introducing line defects which cost no energy. For instance a configura-

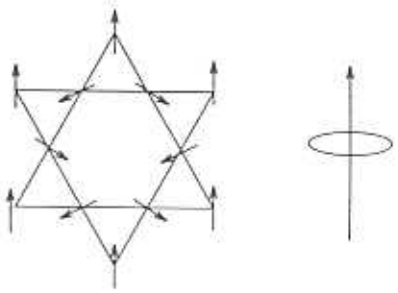

Figure 1.3: Rotating the spins within the hexagon about the axis defined beside the figure generates a degenerate non coplanar state

tion with a closed line connecting spins of one orientation can be deformed by rotating the neighbouring spins about the axis defined by the first spin as in figure 1.3. All non-coplanar configurations can be arrived at starting from different coplanar configurations in this manner.

Calculating the energy cost of small thermal fluctuations about the classical configurations indicates that the states with the largest number of zero modes are favoured at low temperatures. This is a preference of the coplanar states with respect to the non-coplanar states. Further, among the planar states, some special states which will be referred to in forthcoming sections are the so

called $\mathbf{q}$ =0 state and the $\sqrt{3} \times \sqrt{3}$ spiral state of the TLAF which are shown in figure 1.4.

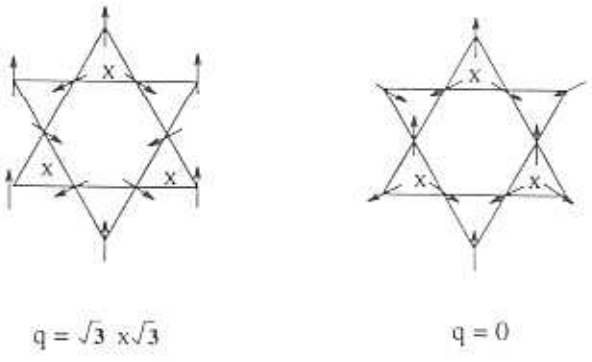

Figure 1.4: Two planar ground states of the KLAF possessing staggered chiral and chiral order respectively

These two states are also special in that they are characterized by different order parameters which are now described. The subset of all coplanar ground states is characterised by the Nematic order parameter [14, 15] which will be described in detail in the following chapters. This is an order parameter that is insensitive to the chirality of the underlying spin configuration and there for does not distinguish between the different coplanar configurations. The chiral order parameter defines the chirality of each triangular plaquette and thus distinguishes between the $\mathbf{q} = 0$ state and the $\mathbf{q} = \sqrt{3} \times \sqrt{3}$ state. So that while the former is characterised by long range chiral order of the elementary triangular plaquettes while the latter is characterised by long staggered chiral

ordering.

This can be seen from figure 1.4 in which the triangular plaquettes are marked out by crosses. Thus $\sqrt{3} \times \sqrt{3}$ order, for instance should show both Nematic order and staggered chiral order while an arbitrary planar state would not posses long range chiral order but would show long range Nematic order. Therefore different candidate ground states of the KLAF may be distinguished by these different order parameters.

1.2.2 Experimental results on the KLAF

The layered compound Sr Cr_{8-x} Ga_{4+x} O_{19} contains antiferromagnetically interacting Cr^{3+} ($S = \frac{3}{2}$) molecules on a Kagome Lattice [16]. Despite a large Curie Weiss temperature of -492 K, long range magnetic order is not seen even up to low temperatures indicating the high degree of frustration. Later specific heat measurements and measurements of magnetic susceptibility indicate that the material undergoes a spin glass transition around 5 K as indicated by the branching of the susceptibility and the difference in the peaking temperatures of the specific heat and susceptibility curves [17, 18]. The low temperature specific heat behaves as T^2 which is unlike what is expected of a spin glass and is more like an indication of gapless magnons in 2-dimensions. This thereby is a signal of a long range ordered state.

However this is contrary to estimates of the correlation length from neutron scattering data. Neutron scattering experiments were performed [19] to probe within the spin glass phase on samples with 80% occupancy of Cr molecules

on the 12 K sites forming the Kagome planes. Elastic neutron scattering data shows a broad peak at the wave vector $Q_0 = 1.4\ A°$, with the associated lowest order superlattice spots falling on $Q_0 = (\frac{1}{3}, \frac{1}{3})$ associated with $\sqrt{3} \times \sqrt{3}$ (3 sublattice) order. Fitting the Q dependent elastic scattering to a 2-dimensional Lorentzian yields a correlation length $\xi \sim 7A°$ which is about twice the inter Cr spacing.

In Deuteronium Jarosite $(D_3O)Fe_3(SO_4)_2(OD)_6$ [20] which is an S= $\frac{5}{2}$ Kagome antiferromagnet features similar to SCGO are seen. Susceptibility measurements show strong in-plane antiferromagnetic exchange suggested by $\theta_{cw} \sim -1500K$ and a spin-glass transition at $T_f = 13.8K$, while the magnetic contribution to the specific heat below T_f rises with T as T^2, characteristic of two-dimensional propagating modes. Neutron diffraction reveals short-range magnetic correlations $\xi \sim 19\mathring{A}$ with a wave vector corresponding to the $\sqrt{3} \times \sqrt{3}$ spin structure at 1.9 K.

On the other hand in the other family of Jarosite compounds containing Chromium, $KCr_3(OD)_6(SO_4)_2$ [21], which are spin $\frac{3}{2}$ KLAF and in the Iron Jarosites $KFe_3(OH)_6(XO_4)_2$ [22] which is a spin $\frac{5}{2}$ (where X = S or Cr) long range order of the $\mathbf{q} = 0$ type is seen.

From the above observations, it appears that while some of the Kagome compounds show long range order, it is tied to the $\mathbf{q} = 0$ order whereas those in which the $\sqrt{3} \times \sqrt{3}$ order is stabilized do not seem to favour long range ordering. The experiments on compounds with short ranged $\sqrt{3} \times \sqrt{3}$ order therefore indicate that the KLAF is either a spin glass with unconventional low

lying excitations or there is long range order in the ground state due to an order parameter insensitive to the neutrons, thereby leading to gapless excitations and a T^2 dependence of the specific heat.

1.2.3 Monte Carlo Analysis of 2-D classical KLAF

The classical KLAF at low temperatures has been studied by Chalker et al and Reimers et al [13, 23]. Chalker et al find that both the spin spin correlations and the Nematic correlation lengths fall by power laws with distance. The Nematic correlation function seems to fall off more slowly than the spin spin correlation function at a temperature of $\frac{T}{J} = 3 \times 10^{-3}$.

Reimers and Berlinsky take up this study further and actually compute the exponents associated with the correlation functions of all of the order parameters described above at a temperature of $\frac{T}{J} \sim 2 \times 10^{-3}$. They obtain different exponents for the Nematic, the 3 state potts, and the $\sqrt{3} \times \sqrt{3}$ correlation functions which are, $\eta_{Nem} = 0.09$, $\eta_3 = 0.16$, $\eta_{\sqrt{3}} = 0.93$ for warming runs from the $\sqrt{3} \times \sqrt{3}$ state and $\eta_{Nem} = 0.71$, $\eta_3 = 0.42$, $\eta_{\sqrt{3}} = 1.4$ for cooling runs. The Chiral order is short ranged, so the $\sqrt{3} \times \sqrt{3}$ state is preferred over the $\mathbf{q} = 0$ state. Further the $\sqrt{3} \times \sqrt{3}$ order seems to be unstable towards the formation of chiral domains, therefore within this framework the ground state is described by large $\sqrt{3} \times \sqrt{3}$ correlated regions separated by domain walls.

1.2.4 Other results on the KLAF

Several semi-classical approaches to the KLAF show evidence for long range $\sqrt{3} \times \sqrt{3}$ order such as the High temperature series expansion of Harris et al [24], the spin wave theory of Chubukov [25]. In contrast to this, the results of exact diagonalization calculations of, [26, 27, 28] indicate that the spin spin correlations decay rapidly with distance. The Ising type series expansions of Singh et al [29] indicate that the KLAF is disordered. The large N expansion starting from an Sp(N) extension of the spin model by [30] also infer that the KLAF is disordered whereas the SU(N) fermionic theory of [31] put forth the idea that the ground state is a chiral spin liquid.

Recent results from exact diagonalization studies on finite sized $J_1 - J_2$ model on the Kagome lattice suggest that this model undergoes a transition from a TLAF like phase with broken spin symmetry to a phase without long range spin order. At the KLAF end there are a series of energy levels with a small gap, approximately forming a continuum, which are expected to collapse to the ground state for the lattice size $N \to \infty$. There is indication however that the symmetry breaking mechanism is of not the kind seen in the TLAF. This is a result that is relevant to this thesis as will become clear when we, now, define our approach to this problem and describe briefly our results.

1.3 About the thesis.

The puzzle posed by the KLAF is that the interplay of quantum fluctuations low dimensionality and frustration appear to create gapless bosonic low en-

ergy excitations over a ground state with no long range spin order. This is seen in the experiments of Deuteronium Jarosite and on SCGO. Both these compounds show very short ranged $\sqrt{3} \times \sqrt{3}$ order as inferred from neutron scattering data. The low temperature specific heat capacity behaves like T^2 which contrary to the indications of the neutron scattering data are reminiscent of an underlying ordered state with gapless bosonic excitations. The natural question to ask therefore is concerning the mechanism by which this gapless mode comes into existence when there is no long range spin order. One possibility that have been put forth in this context is that it is a spin Nematic, having long range order in the second rank nematic tensor order parameter.

In this thesis we approach the KLAF from the $\sqrt{3} \times \sqrt{3}$ ordered state. In order to do this, we study a family of models that interpolate between the KLAF and the TLAF for values of a parameter χ. These models share the $\sqrt{3} \times \sqrt{3}$ state as the unique minimum energy configuration. The KLAF of course has in addition all the other degenerate ground states described above and this is really an approach from the $\sqrt{3} \times \sqrt{3}$ end, with the TLAF itself serving as a reference point where we formulate the renormalization group theory and the large N expansion.

We describe these models by $SO(3)_R \times SO(2)_L$ nonlinear σ model field theory and probe the ground state and low energy excitations of the models within this description. We see that near the TLAF these models are described by theories such as the ones studied in [10] where the dominant fields are the three goldstone modes which arise due to the breaking of the spin rotational symmetry. Near the KLAF there are in addition to the three goldstone modes,

two modes which are described by a unit vector field $\vec{m}$. The interaction between them drives the system for a range of parameters into a phase where the spin symmetry is completely restored but the $SO(2)_L$ symmetry is broken leading to one gapless excitation. Thus the phase diagram of the model as the parameter χ is varied from 1 to 0 is that initially there is a state with long range $\sqrt{3} \times \sqrt{3}$ order which gives way at intermediate χ to a phase with all symmetries unbroken and finally near $\chi \rightarrow 0$ there is a novel phase with the $SO(3)_R$ symmetry intact but with the $SO(2)_L$ symmetry being broken. At the level of microscopic model this is interpreted in terms of long range order in the order parameter $\vec{S}_1.\vec{S}_2 \times \vec{S}_3$. Further we see that the Nematic and the Spin correlations are characterised by different length scales.

The break up of the problem which describes our approach is as follows,

- In Chapter 2 we introduce the spin models that we plan to study and identify the relevant low energy modes by making a Holstein - Primakoff spin wave expansion about the classical ground state.

- In Chapter 3 we describe the derivation of the field theory from the microscopic model of the sector close to the TLAF and analyse the theory by a renormalization group calculation to probe the nature of the ground state dominated by the goldstone modes.

- In Chapter 4 this analysis is repeated for models close to the KLAF and we show that there exists a phase close to the KLAF where there is the breaking of the $SO(2)_L$ symmetry in the spin disordered phase.

- Chapter 5 carries the summary of our study and here we interpret the result of earlier chapters to form our conclusions about the ground state of the KLAF which we have described above.

Chapter 2

From the Triangular to the Kagome Lattice

In this chapter, we describe the results of a semiclassical spin wave analysis on a family of antiferromagnetic spin models which extrapolate from the Kagome to the Triangular Lattice Models for values of a real parameter χ varying from 0 to 1. This is also an approach to studying large frustrating interactions on the $\sqrt{3} \times \sqrt{3}$ state as described in the introductory chapter. The relevant modes, which describe the physics near the triangular lattice (TLAF) end are the three gapless goldstone modes which correspond to the breakdown of the SO(3) spin symmetry of the Hamiltonian. In a semiclassical picture, they represent rigid rotations of the spins on the unit cell. Near the KLAF, we identify two other branches with a small gap which vanishes for $\chi = 0$. Fluctuations in these modes are shown to become relevant for small χ by computing their contribution to the reduction in magnetization. The Staggered Chiral and The Nematic order parameters are also studied in this approximation with a view to seeing if there exists a regime where these types of order can exist in the absence of Magnetization. In the last section, we derive a parametrisation for these extra modes.

2.1 The Model and Classical Ground states

In this section we define a Heisenberg antiferromagnetic (HAF) spin model with nearest neighbour interactions defined on a triangular lattice. The exchange parameters J_{ij} are functions of a real parameter χ so that when $\chi = 0$ the model is geared to mimic the HAF on a Kagome Lattice (KLAF). When $\chi = 1$ this model reproduces the TLAF. For arbitrary χ, we call this the Deformed Triangular Lattice Antiferromagnet (DTLAF) for brevity. This model has also been studied by [24] we however study it only with a view to obtaining a parametrisation of the relevant low lying modes. This model is given by the Hamiltonian,

$$H = \sum_{<i,j>} J_{ij} \, \vec{S}_i . \vec{S}_j \tag{2.1}$$

Writing out J_{ij} explicitly,

$$H = J \, (\sum_{<i,j> \epsilon K_B} \vec{S}_i . \vec{S}_j + \chi \sum_{<i,j> \not\epsilon K_B} \vec{S}_i . \vec{S}_j \;) \tag{2.2}$$

The labels i, j in the above expressions refer to the sites on a parent triangular lattice of which $\frac{1}{4}$ are the non-Kagome points. The first term is a sum over nearest neigbours connected by Kagome bonds denoted by K_B and which are indicated by solid lines in figure 2.1, and the second term involves a sum over those i and j which are connected by non-Kagome bonds, indicated by dotted lines in the figure. In this section we will be dealing only with the classical spin model, therefore the spins $\vec{S}_i$ are classical vectors constrained to obey the relation $\vec{S}_i . \vec{S}_i = S^2$.

We determine the classical ground states of this model for various ranges of χ. We begin with the parameter range $0 < \chi < 2$ where the total energy

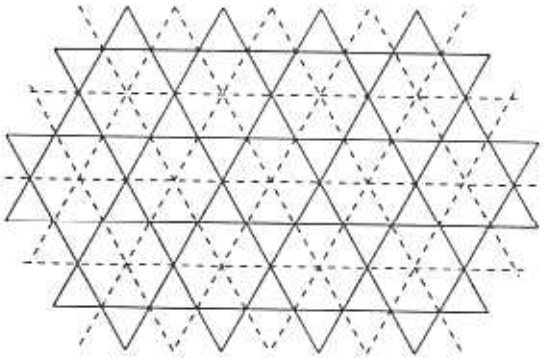

Figure 2.1: The DTLAF : The Non-Kagome bonds are shown as dotted lines and the Kagome bonds are shown in bold lines

of the system described by the Hamiltonian in equation (2.2) can be rewritten as,

$$\frac{E}{J} = \frac{1}{2}\left(1 - \frac{\chi}{2}\right)\sum_{\Delta_K}\left(\sum_{i=1}^{3}\vec{S}_i\right)^2 + \frac{\chi}{4}\sum_{\Delta_{NK}}\left(\sum_{i=1}^{3}\vec{S}_i\right)^2 - \frac{3S^2N}{2}\left(\frac{1+\chi}{2}\right) \qquad (2.3)$$

Where N is the total number of sites in the parent TL and the first term is summed over the spins belonging to those triangles Δ_K which are bounded by three solid lines and which lie on the KL points only and the second term is summed over the triangles Δ_{NK} which are bounded by two dashed lines and which lie on points not belonging to the KL.

In this range of χ, the coefficients of the first two terms in equation (2.3) are positive. Thus the energy is minimized by spin configurations that satisfy

the condition that the net magnetization of every triangular plaquette, i.e $(\vec{S}_1 + \vec{S}_2 + \vec{S}_3)$ is zero. For non-zero values of λ lying in this range, the unique solution of this constraint is, up to symmetry operations, the so called $\sqrt{3} \times \sqrt{3}$ state.

Shown in figure 2.2, this is a structure made up of three sublattices, labelled A, B and C, populated by the spins S_A, S_B and S_C respectively.

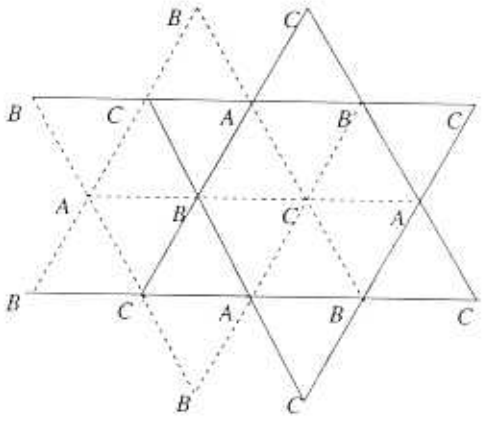

Figure 2.2: Ground State of the DTLAF for the range $0 < \lambda < 2$

One specific choice for this which we will use in following calculations is given by,

$$\begin{aligned} \vec{S}_A &= \hat{X} S \\ \vec{S}_B &= [-\frac{1}{2}\hat{X} + \frac{\sqrt{3}}{2}\hat{Y}]S \end{aligned}$$

which fixes for us, $$\vec{S}_C = [-\frac{1}{2}\hat{X} - \frac{\sqrt{3}}{2}\hat{Y}]S \tag{2.4}$$

Apart from global rotations and reflections about the three component spins $\vec{S}_A, \vec{S}_B$ and $\vec{S}_C$ this is the unique solution to the minimum energy condition. However at $\chi = 0$, there are many other solutions which satisfy the constraint $\sum \vec{S}_i = 0$ for each triangular plaquette. This results in the huge degeneracy of the Ground states consisting of planar and non-planar configurations that were described in section (1.4) .

The ground state energy in this range of χ is given by ,

$$E_{G.S} = -\frac{3JNS^2}{4}\left(\frac{1+\chi}{2}\right) \tag{2.5}$$

The above range of χ is the one that is relevant to ensuing discussions but we present here the calculations for the Ground states of the DTLAF for $\chi > 2$ which also show interesting structure.

For instance in the range $\chi \geq 2$ we rewrite the energy as,

$$\frac{E}{J} = \sum_{\Delta_{NK}} \frac{1}{2}\left(\vec{S}_{1K} + \vec{S}_{2K} + \frac{\chi}{2}\vec{S}_{NK}\right)^2 - \frac{3S^2N}{2}\left(1 + \frac{\chi^2}{8}\right) \tag{2.6}$$

where the sum is over all the non-Kagome triangles Δ_{NK} made up of two Kagome points and one non-Kagome point. $\vec{S}_{1K}$ and $\vec{S}_{2K}$ are the spins at these two Kagome sites and $\vec{S}_{NK}$ is the spin at the non-Kagome site at the centre of every hexagon.

In the range $2 \leq \chi \leq 4$, the quantity $(\vec{S}_{1K} + \vec{S}_{2K} + \frac{\chi}{2}\vec{S}_{NK})$ can be made to be equal to zero on every triangle by a non-coplanar spin configuration described below. We can define this state with respect to the $\sqrt{3} \times \sqrt{3}$ state of Figure 2.2 as follows. Consider such a triangle in which the non-Kagome site has the spin $\vec{S}_c$ lying on it and let $\vec{S}_A$ and $\vec{S}_B$ be the spins on the other two Kagome sites. We can construct on this base the linear combination which will minimise the energy equation, as follows.

Let
$$\begin{aligned} \vec{S}_{1K} &= \cos\theta\vec{S}_A + S\sin\theta\hat{z} \\ \vec{S}_{2K} &= \cos\theta\vec{S}_B + S\sin\theta\hat{z} \end{aligned}$$

and
$$\begin{aligned} \vec{S}_{NK} &= -\frac{2}{\chi}\left(\vec{S}_{1K} + \vec{S}_{2K}\right) \\ &= \frac{2}{\chi}\left(\cos\theta\vec{S}_C - 2S\sin\theta\hat{z}\right) \end{aligned} \tag{2.7}$$

This minimises the expression (2.6) when θ satisfies the equation

$$\sin^2\theta = \frac{1}{3}\left(\frac{\chi^2}{4} - 1\right) \tag{2.8}$$

for every triangle under consideration. Equation (2.8) always has a solution in the parameter range $2 \leq \chi \leq 4$. Thus the non-coplanar configuration described in equations (2.7) is the stable ground state in this range of χ. The ground state energy in this range is given by,

$$E_{G.S} = -\frac{3S^2JN}{2}\left(1 + \frac{\chi^2}{8}\right) \tag{2.9}$$

At $\chi = 4$, we have $\theta = \pi/2$. All the spins are then collinear. The spins on the Kagome lattice point up and the others point down. Examining the energy

as written in equation (2.6), it is clear that this state ($\theta = \pi/2$) will minimize the energy in the range $\chi \geq 4$. The ground state energy in this range being,

$$E_{G.S} = -\frac{3S^2JN}{2}(\chi - 1) \tag{2.10}$$

In the range $\chi > 2$, the system has non-zero magnetization. The average magnetization per site is given by,

$$\begin{aligned} \vec{M} &= S\sin\theta\left(\frac{3}{4} - \frac{1}{\chi}\right)\hat{z} \qquad 2 \leq \chi \leq 4 \\ &= \frac{S}{2}\hat{z} \qquad\qquad\qquad\qquad \chi \geq 4 \end{aligned} \tag{2.11}$$

To summarize the above, we have defined the DTLAF and derived expressions for the classical ground states of this model. We find that the models fall into three categories depending on the value of χ as follows,

- The range $0 \leq \chi < 2$ where the ground state is the planar spiral state with spiral angle = 120 °, unique up to symmetry operations.
- The range $2 < \chi < 4$ where the spins start lifting off the plane. The spins on the Kagome sites having a $\hat{z}$ component which is anti parallel to the $\hat{z}$ component of the spins on the non-Kagome sites. This state is thus a combination of a spiral and ferrimagnetic state.
- At χ= 4 all the spins are collinear and the transition to the ferrimagnetic state is complete. The ferrimagnetic state persists for all the values of

$\chi \geq 4$.

2.2 Inclusion of Fluctuations: Linear Spin wave theory

In this section, we calculate the leading order corrections to the classical Neel state due to quantum fluctuations in the linear spin wave approximation. In this approximation the spin operators are mapped on to bosonic creation and annihilation operators through the Holstein Primakoff transformation. This mapping is exact in the limit of S$\rightarrow \infty$ and for a finite S it is to be understood that these operators act on a finite dimensional Hilbert space. First applied to quantum antiferromagnets on bipartite lattices by Anderson ([1]), this mapping is a good semiclassical approximation for $zS \gg 1$, where z is the co-ordination number of the lattice.

First we present the spin wave analysis of the DTLAF about the $\sqrt{3} \times \sqrt{3}$ classical configuration which has been described in the previous section. Referring again to figure (2.2) we see that the minimal unit cell we can construct that takes into account the periodicity of the ground state and that of the Hamiltonian consists of 12 lattice points. Each lattice point is labelled by 3 indices (I,i,α), where $\vec{I}$ is the vector associated with the particular unit cell to which the point belongs and (i, α) label the points within each unit cell as shown in figure 2.3 which shows one choice of the unit cell. With this notation in mind, the classical ground state configuration of figure 2.2, may be written as, $\vec{S}^{cl}_{Ii\alpha} = S\hat{n}_\alpha$, where $\hat{n}_0 = (1,0,0), \hat{n}_1 = (-\frac{1}{2}, \frac{\sqrt{3}}{2}, 0)$ and $\hat{n}_2 = (-\frac{1}{2}, -\frac{\sqrt{3}}{2}, 0)$

and the Hamiltonian can be written as

$$H = \sum_{I i\alpha, J j\beta} \frac{1}{2} J_{I i\alpha, J j\beta} Tr[\mathbf{S}_{I i\alpha} \mathbf{S}_{J j\beta}] \tag{2.12}$$

In the above expression the J_{ij} have been rewritten suitably as the Matrix $J_{Ii\alpha,Jj\beta}$. The explicit form of $J_{Ii\alpha,Jj\beta}$ is not given here but will be given along with the calculation at a later stage. Here, in order to facilitate our calculation, we have rewritten the $\vec{S}_{Ii\alpha}$ as $\mathbf{S}_{Ii\alpha} = \vec{S}_{Ii\alpha}.\vec{\tau}$, where $\vec{\tau}$ are the Pauli matrices. Including the effects of quantum fluctuations consists of rotating this spin

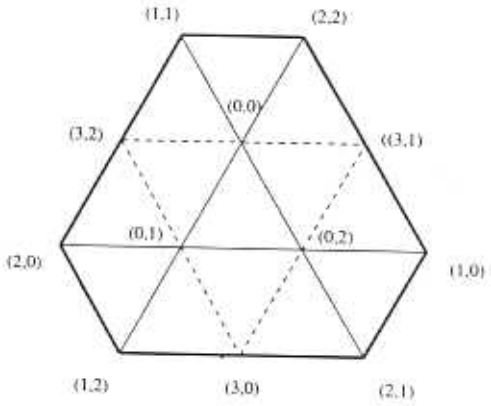

Figure 2.3: Unit Cell with 12 lattice points labelled by (i, α) as shown

from its classical value by a unitary transformation as follows,

$$\mathbf{S}_{Ii\alpha} = \tilde{s}\ U^{\dagger}_{Ii\alpha} \mathbf{n}_{\alpha} U_{Ii\alpha} \tag{2.13}$$

Where for small fluctuations the $U_{Ii\alpha}$ can be expressed as,

$$U_{Ii\alpha} = \exp(\frac{i}{2\sqrt{\tilde{s}}} w_{Ii\alpha}) \tag{2.14}$$

with the w representing fluctuations of the spins and being given by,

$$w_{Ii\alpha} = p_{Ii\alpha}\epsilon_\alpha + q_{Ii\alpha}\tau^3 \tag{2.15}$$

Here, $\{\hat{n}_\alpha, \hat{\epsilon}_\alpha, \hat{z}\}$ form an orthonormal set of basis vectors defined on each sublattice, in terms of which we express the spins. The operators $p_{Ii\alpha}, q_{Ii\alpha}$ satisfy the algebra $[p_{Ii\alpha}, q_{Ii\alpha}] = -i\hbar$. Equation (2.13) gives the mapping from spin variables to bosonic variables and is equivalent to the Holstein Primakoff transformation. This is apparent in the following expansion of $S_{Ii\alpha}$ along the basis vectors $\{\hat{n}_\alpha, \hat{\epsilon}_\alpha, \hat{z}\}$, in which we have kept the terms up to order $\frac{1}{\tilde{s}}$.

$$\mathbf{S}_{Ii\alpha} = \tilde{s}[n_\alpha(1 - \frac{1}{2\tilde{s}}(p_{Ii\alpha}^2 + q_{Ii\alpha}^2)) - p_{Ii\alpha}\tau^3 + q_{Ii\alpha}\epsilon_\alpha] \tag{2.16}$$

This is exactly the first order approximation to the Holstein Primakoff transformation adapted to fluctuations about the $\sqrt{3} \times \sqrt{3}$ configuration.

In this expansion, $\tilde{s}$ sets the scale by which to make a perturbative order by order calculation. Therefore substituting for $S_{Ii\alpha}$ in the hamiltonian with the expression (2.16) we get the following expression for the fluctuations hamiltonian which contains quantum corrections of order $\frac{1}{\tilde{s}}$.

$$H = \frac{\tilde{s}^2}{2} \sum_{Ii\alpha, \mathbf{J}j\beta} J_{Ii\alpha, Jj\beta} Tr[-\frac{1}{2\tilde{s}} n_\alpha n_\beta ({w_{Ii\alpha}}^2 + {w_{Jj\beta}}^2) - \frac{1}{\tilde{s}} w_{Ii\alpha} n_\alpha w_{Jj\beta} n_\beta] \tag{2.17}$$

where,

$$\mathbf{J}_{Ii\alpha, Jj\beta} = \delta_{I,J} J^0_{i\alpha, j\beta} + \frac{1}{2} \sum_{r=1,3} [\delta_{J,I+E_r} J^r_{i\alpha, j\beta} + \delta_{J,I-E_r} (J^r)^T_{i\alpha, j\beta}] \tag{2.18}$$

In the above expression the vectors $\hat{E}_r$ connect the unit cell to corresponding points on adjacent unit cells. $\hat{E}_1 = 2\sqrt{3}(0, -1, 0), \hat{E}_2 = 2\sqrt{3}(\frac{\sqrt{3}}{2}, \frac{1}{2}, 0)$ and $\hat{E}_3 = -(\hat{E}_1 + \hat{E}_2)$. The expressions for J^0 and J^r are given in Appendix A.

The spin wave co-ordinates $p_{Ki\alpha}$ and $q_{Ki\alpha}$ are defined as follows,

$$p(q)_{Ki\alpha}i = \frac{1}{\sqrt{N}}\sum_{I} p(q)_{Ii\alpha}\exp\left(-i\vec{K}.\vec{I}\right) \tag{2.19}$$

The sum is over the superlattice of vectors $\vec{I}$ and $\vec{K}$ are the corresponding reciprocal lattice vectors. Rewriting H in terms of these spin wave variables we get,

$$H = \frac{J\bar{s}}{8}\sum_{K,i\alpha,j\beta}\left[p_{-Ki\alpha}M^{-1}_{i\alpha,j\beta}p_{Kj\beta} + q_{-Ki\alpha}K_{i\alpha,j\beta}q_{Kj\beta}\right] \tag{2.20}$$

where the 12×12 matrices M^{-1} and K are given in the appendix-A.

Since M^{-1} and K do not commute for arbitrary χ, we cannot diagonalise the hamiltonian by a simple unitary transformation. Instead we obtain the set of left and right eigenvectors of $\Delta\Omega^2 = M^{-1}K$ and express the hamiltonian in this basis to get the final diagonal form. First, we define the P_{Knr} as follows,

$$\begin{aligned} p_{Ki\alpha} &= \sum_{nr}\Phi^{nr}_{Ri\alpha}P_{Knr} \\ q_{Ki\alpha} &= \sum_{nr}\Phi^{nr}_{Li\alpha}Q_{Knr} \end{aligned} \tag{2.21}$$

The columns of the matrices $\Phi^{nr}_{Ri\alpha}$ and $\Phi^{nr}_{Li\alpha}$ are the $\psi_{Ri\alpha}$ (or $\psi_{Li\alpha}$) which are the Right (or Left respectively) eigenvectors of Ω^2 and are given in appendix A.2. The vectors ψ satisfy the following orthogonality relations,

$$\psi^{\dagger nr}_{L}, \psi^{n'r'}_{R} = \delta_{n,n'}\delta_{r,r'} \tag{2.22}$$

$$\psi^{\dagger}_{Li\alpha}, \psi_{Ri'\alpha'} = \delta_{i,i'}\delta_{\alpha,\alpha'} \tag{2.23}$$

Using the transformation equations (2.21) we can see that like the p and q, the P s and the Q s obey the canonical commutation rules,

$$[Q_{Knr}, P_{-Kn'r'}] = i\delta_{n,n'}\delta_{r,r'} \tag{2.24}$$

Expressed in this basis, H takes the form,

$$H = \sum_{n,r} \frac{1}{8}[c_{nr} P_{nr}^2 + c'_{nr} Q_{nr}^2] \tag{2.25}$$

We rescale the $P_{n,r}$ and $Q_{n,r}$ to write this in a standard form, as,

$$H = \frac{1}{2} \sum_{nr} \omega_{nr} (\tilde{P_{nr}}^2 + \tilde{Q_{nr}}^2) \tag{2.26}$$

where

$$\begin{aligned} \tilde{P_{nr}}^2 &= \frac{1}{4} \frac{\omega_{nr}}{c'_{nr}} P_{nr}^2 \\ \tilde{Q_{nr}}^2 &= \frac{1}{4} \frac{\omega_{nr}}{c_{nr}} Q_{nr}^2 \end{aligned} \tag{2.27}$$

The eigenvalues and eigenvectors of the matrix Ω^2, which are given in the appendix A.2, indicate that these modes fall into three categories which we call the H-H, H-S, and the S-S modes as follows using the conventions of appendix A to label the modes.

- The modes (0,0), (0,1), (0,2) are the soft modes, gapless for all χ, which we shall address as the S-S modes.
- The modes (1,0), (1,1), (3,1), (1,2), (3,2), which are hard for non-zero χ but become gapless for $\chi = 0$, will be referred to as the H-S modes.
- The modes (2,0), (3,0), (2,1), (2,2), which remain hard for all χ will be referred to as the H-H modes.

Among the H-S modes, there are two groups. The modes (1,0) , (1,1) and (1,2), are spurious degrees of freedom at $\chi = 0$ as they decouple the Kagome points from the rest of the lattice at this point. The modes (3,1) and (3,2) on the other hand, are the ones which truly soften and become gapless at $\chi = 0$.

2.3 Order Parameter reduction to order $\frac{1}{S}$

Now that we have a parametrisation of the soft and hard modes of the system, we can define suitable order parameters to characterize the ground state and calculate the reduction in these order parameters from their classical values due to quantum fluctuations within the spin wave approximation. The various order parameters that we study in this section are the staggered Magnetization M, the staggered Chiral order parameter C and the components of the Nematic Tensor Σ_{ij}^{ab}. This reduction is used to get an estimate of S_{cr} as that value of S where the fluctuations destroy the order. Of these order parameters the Neel magnetization M is the most natural choice, the others that we have mentioned above are interesting in the context of the KLAF. It has been proposed in the context of the KLAF that being a spin nematic, the system shows the long range ordering of the second rank tensor Σ.

With a view to writing these operators in our notation, we first define three orthogonal vectors, $\mathbf{n}^a$ as follows,

$$n_k^1 = \frac{\tilde{s}}{12}\sum_{i,\alpha}\frac{1}{2}Tr\{\tau^k U_{i\alpha}^\dagger \tau^1 U_{i\alpha}\} \tag{2.28}$$

$$n_k^2 = \frac{\tilde{s}}{12}\sum_{i,\alpha}\frac{1}{2}Tr\{\tau^k U_{i\alpha}^\dagger \tau^2 U_{i\alpha}\} \tag{2.29}$$

$$n_k^3 = \frac{1}{24i}\frac{2}{\sqrt{3}}\sum_{i,\alpha}\frac{1}{2}Tr\{\tau^k [\mathbf{S}_{i\alpha}, \mathbf{S}_{i\alpha+1}]\} \tag{2.30}$$

Of the above, $\mathbf{n}^1$ is the same as the average Staggered Magnetization, M_I, per unit cell, $\mathbf{n}^2$ is perpendicular to it and $\mathbf{n}^3$ is also known as the staggered Chiral order parameter C_I. The $\mathbf{n}^a$ are 3 orthogonal vectors each of which carries an index k. The right transformations $SO(3)_R$ act on the index a and cause a mixing among these. The left rotations $SO(2)_L$ are transformations that act on the index k. This additional symmetry $SO(2)_L$ is a symmetry present in the spin wave theory which makes the two spin wave velocities equal. Under the $SO(2)_L$ transformations, $\mathbf{n}^1$ and $\mathbf{n}^2$ transform as doublets and $\mathbf{n}^3$ is invariant. A Symmetric rank 2 tensor that we can construct out of these forms is the Nematic tensor which is defined as follows,

$$\Sigma_{i,j}^{a,b} = \frac{1}{\sqrt{6}}\left[n_i^a n_j^b - \delta_{ij}\sum_k n_i^k n_i^k\right] \tag{2.31}$$

Of these, $\mathbf{\Sigma}^{33}$ is generally referred to as the Nematic order parameter $\mathbf{N}$. This is a singlet under the $SO(2)_L$ transformations and has the quantum numbers (2,0) associated with the action of $SO(3)_R$. The correlations of $\mathbf{N}_I$ are a measure of the planarity of the spins of the ground state. For instance in the classical $\sqrt{3}\times\sqrt{3}$ state this has the maximum value, normalised to be 1.

We have calculated the reduction of M_I, C_I and N_I due to the inclusion of quantum fluctuations to the background spiral state and find that the ordering

is more strongly suppressed for N_I as compared to C_I as compared to M_I. To give the salient features of this calculation,

Approximating $\mathbf{M}_I$ to order $\frac{1}{\tilde{s}}$, we have,

$$M_I = \frac{\tilde{s}}{12}\sum_{i\alpha}[\tau^1 - \frac{i}{\sqrt{\tilde{s}}}w_{Ii\alpha}\tau^1 - \frac{1}{2\tilde{s}}{w_{Ii\alpha}}^2\tau^1] \tag{2.32}$$

$$\text{and} \qquad < M_I >= M_I^{cl}(1 - \frac{1}{s}\triangle M_I) \tag{2.33}$$

where $\mathrm{M}_I^{cl} = S\tau^1$ and $\triangle M_I$ is in terms of the fourier modes ${w_{Ki\alpha}}^{1}$,

$$\triangle M_I = \frac{1}{24}\sum_{a,i,\alpha}[\int \frac{d^2K}{V_b}[< {w_{Ki\alpha}}^a w_{-Ki\alpha}{}^a > -1] \tag{2.34}$$

In order to see how they act in reducing the staggered magnetization for different ranges of χ we calculate separately the contributions of all the soft modes which are labelled by (n,r) = (0,0), (0,1) and (0,2). In the case of the hard modes we approximate the dispersion relation by neglecting the k dependence and in the case of the soft modes the dispersion is taken to be, $\omega_{nr} = V_{nr}$ k. These separate contributions are given by, below,

$$\triangle M_I^{nr} = \left\{\left[\Phi_{R,i\alpha}^{*nr}\Phi_{R,i\alpha}^{nr}\frac{c'_{nr}}{V_{nr}\Lambda} + \Phi_{L,i\alpha}^{*nr}\Phi_{L,i\alpha}^{nr}\frac{V_{nr}\Lambda}{3c'_{nr}}\right] - 1\right\} \tag{2.35}$$

For (n,r) = (0,0):

$$\triangle M_I^{nr} = \left\{\left[\Phi_{R,i\alpha}^{*nr}\Phi_{R,i\alpha}^{nr}\frac{V_{nr}\Lambda}{3c_{nr}} + \Phi_{L,i\alpha}^{*nr}\Phi_{L,i\alpha}^{nr}\frac{c_{nr}}{V_{nr}\Lambda}\right] - 1\right\} \tag{2.36}$$

In the same way, we calculate separately the contribution to $\triangle M_I$ coming from each of the hard modes (H-H and H-S) in which (n,r) take all values except for the above three and this is given by,

[1]Where the fact that $< w_{ki\alpha}^a w_{qi\alpha}^a >$ is non-zero only when $k = -q$ has been used

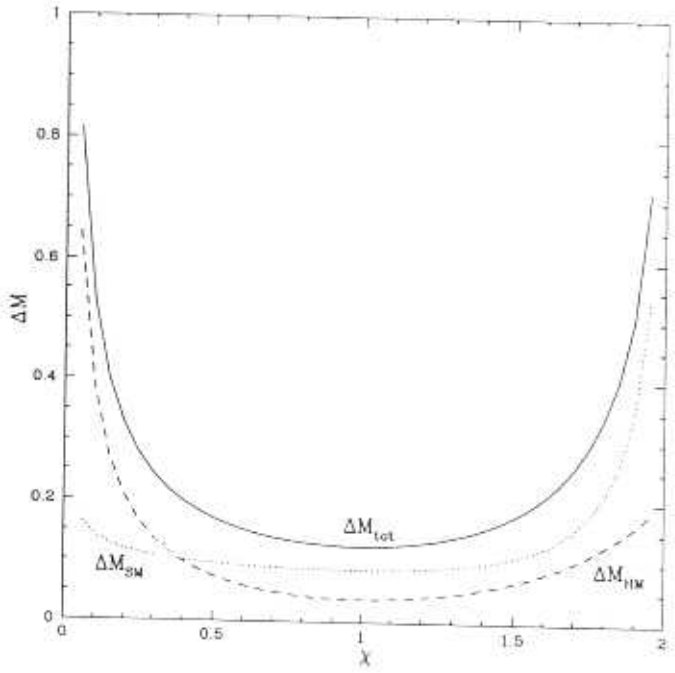

Figure 2.4: Reduction in staggered magnetization due to spin waves plotted as a function of χ showing separately the contributions of the goldstone modes and the other modes.

$$\triangle M_I^{nr} = \frac{1}{2}\left\{\left[\Phi_{R,io}^{*nr}\Phi_{R,io}^{nr}\sqrt{\frac{c'_{nr}}{c_{nr}}} + \Phi_{L,io}^{*nr}\Phi_{L,io}^{nr}\sqrt{\frac{c_{nr}}{c'_{nr}}}\right] - 1\right\} \tag{2.37}$$

We do see a difference in the behaviour of these modes at different ranges of χ as we expected. Thereby, separate contributions of the Hard and soft modes to ΔM_I are shown in figure 2.4 where we see that the dominant quantum fluctuations near $\chi = 1$ are due to the S-S modes, but near $\chi = 0$ the contribution from the H-S modes to ΔM increases considerably. This indicates that the H-S modes could become relevant degrees of freedom while describing the

models close to the KLAF.

We repeat the above calculation for the Chiral order parameter C_I and the Nematic Tensor which has been defined in equation (2.31), in order to see if the presence of the H-S modes alters the ground state order by showing a preference for any of these order parameters. The average value of C_I in the above approximation is given by the expression,

$$< C_I > = C_I^{cl} \left\{ 1 - \frac{1}{12S} \sum_{i\alpha} \int \frac{d^2K}{V_b} < w_{Ki\alpha}{}^2 w_{ki\alpha+1}^2 > \right.$$

$$\left. - \frac{2}{S} \triangle M_I \right\} \tag{2.38}$$

$$\text{where } C_I^{cl} = \frac{\sqrt{3}}{2} S^2 \tau^3 \tag{2.39}$$

The above expressions are plotted as a function of χ and we see that the behaviour is very similar to that of the staggered magnetization. This is because the first factor in equation (2.39) is proportional to $\triangle M$, the coefficient is twice that for $< M_I >$ as seen from (2.33). Further the last term in (2.39) is smaller in magnitude when compared to $\triangle M$, which explains the similarity in the shapes of the two curves shown in figure 2.4 and figure 2.5. We have also calculated the spin wave corrections to Σ^{11} and Σ^{33} and find a similar behaviour and the ordering is even more strongly suppressed.

This completes the spin wave analysis of the DTLAF which has been motivated only by the desire to identify the relevant fluctuations for different

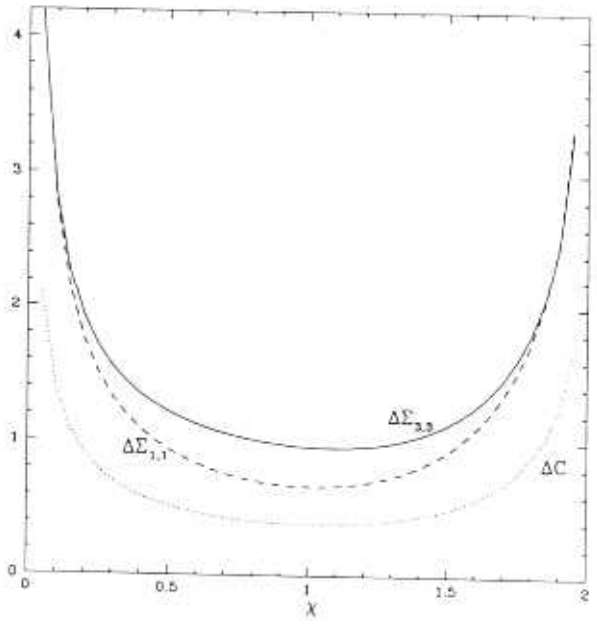

Figure 2.5: Reduction due to spin waves in the classical value of the Chiral order C , the components Σ_{33} and Σ_{11} of the Nematic Tensors shown as a function of χ.

values of χ lying in the range $0 < \chi < 1$. The case of $\chi \sim 1$ is simple since it is not a singular point and we can make a straightforward extension of this representation to that end. We treat the $\chi = 0$ end with a little more care and derive an alternate representation of the H-S modes in the following section, starting from a slightly different model.

2.4 Reparametrising the H-S modes

We introduce here another model which is relevant for our study, which we dub the J_1 - J_2 model, for convenience. In this model, bonds connecting nearest neighbours on the KL have a strength J_1 and within each hexagon, every site

is ferromagnetically coupled to three other sites as shown in figure 2.6 with a strength J_2. This model is equivalent to the DTLAF after integrating out the central Non-Kagome Spin. The Hamiltonian which describes this model can be written as follows.

$$H = J_1 \sum_{<i,j>} \vec{S}_i.\vec{S}_j - J_2 \sum_{\{i,j\}} \vec{S}_i.\vec{S}_j \qquad (2.40)$$

where the first term is the usual sum over the nearest neighbours on the KLAF and the second term represents sums over pairs (i,j) connected by dashed lines in figure 2.6.

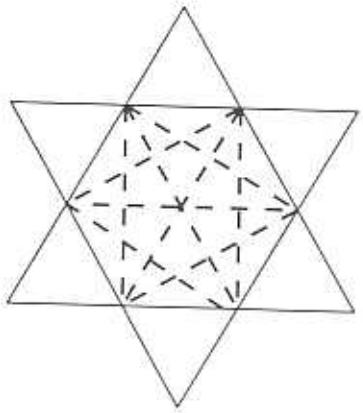

Figure 2.6: The J_1 - J_2 Model on the KLAF - Figure showing the bonds within each hexagon of strength J_2

The spin wave theory of this model is done along the same lines as in the preceding section so we do not present the details here but merely write down the eigenvectors, and indicate those which describe the H-S modes.

The eigenvectors of the $\mathbf{K} = 0$ fluctuations hamiltonian are $\Phi_{j,\beta} = \phi_j \times \phi_\alpha$,

where

$$\begin{aligned}\phi_0 &= \frac{1}{\sqrt{3}}(1,1,1)\\ \phi_1 &= \frac{1}{\sqrt{3}}(1,\alpha,\alpha^2)\\ \phi_2 &= \frac{1}{\sqrt{3}}(1,\alpha^2,\alpha)\end{aligned} \tag{2.41}$$

Of these, the modes are Φ_{11} and Φ_{22} have a gap $\Delta_0 = 3J_2\,(3J_1{+}6\,J_2)$ which vanishes for $J_2 = 0$ and they correspond to the H-S modes.

The labelling of spins on the unit cell which in this case consists of 9 points is as in the case of the DTLAF and is shown in figure 2.7. Small fluctuations

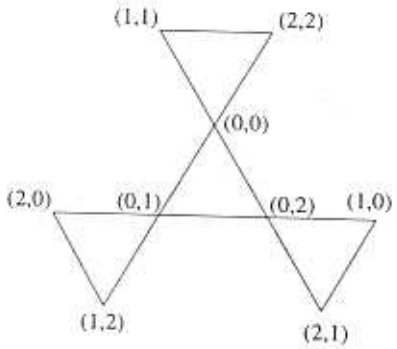

Figure 2.7: The unit cell for the J_1 -J_2 Model on the KLAF - showing the way the spins are labelled

of the classical ground state configuration due to the H-S modes can be written using equation (2.13) as follows,

$$S_{I\alpha} = \check{s}n_\alpha + i\sqrt{\check{s}}[n_\alpha, w_{I\alpha}] \tag{2.42}$$

where the $w_{Ii\alpha}$ defined here is that part of the fluctuations which contain only those H-S modes $P_{11}\Phi_{11}$ and $P_{22}\Phi_{22}$.

$$w_{Ii\alpha}i = [P^{+}\Phi^{i\alpha}_{1,1} + P^{-}\Phi^{i\alpha}_{2,2}]\epsilon^{1}_{\alpha} \tag{2.43}$$

with $P^{+} = (P\ )^{*} = P_1 - iP_2$.

In the following expression, we write down the change in each spin, $\delta S_{i\alpha}$ and choose the subset of states with $\delta S_{i\alpha} = 0$ for $i + \alpha = 0$ (Mod 3) with reference to figure 2.7. Putting this condition in, we get the value of the fluctuation in the other spins to be,

$$\delta S_{Ii\alpha} = \frac{\sqrt{3}\Delta}{\sqrt{s}}\tau^{3} \text{ for i} + \alpha = 1 \tag{2.44}$$

$$\delta S_{Ii\alpha} = \frac{-\sqrt{3}\Delta}{\sqrt{s}}\tau^{3} \text{ for i} + \alpha = 2 \tag{2.45}$$

From the above expressions we see that the $\sum_{\alpha} S_{\alpha} = 0$ for each triangle. The axis of rotation is however different for different triangles thereby creating non-planar configurations. Therefore these modes also represent rigid rotations of the spins on sites $i + \alpha = 1$ and $i + \alpha = 2$ about the axis determined by the spins $i + \alpha = 0$. This generates non-planar configurations even starting from a planar configuration which increases the stiffnesses associated with the other goldstone modes.

This also shows explicitly that for small fluctuations there is no cost of energy due to these excitations. In Chapter (4), we map these modes on to unit vector fields in order to incorporate large fluctuations and study the effects

of the interaction between these modes and the goldstone modes in determining the ground state of the system.

Chapter 3

Field Theory of the DTLAF near $\chi = 1$

In this Chapter we derive the effective field theory of the goldstone modes of DTLAF in the low energy long wavelength approximation starting from the microscopic model. Through a one loop Renormalization Group (R.G) calculation we probe the parameter space near the critical couplings to get the R.G. flow diagram of the model and thereby estimate the phase boundary separating the ordered from the disordered regimes. This is used to obtain the critical value of spin S_{crit} above which the system is ordered. We see that for models with χ close to one, this value is about 0.028 thereby placing the models well within the ordered phase even for S= 1/2.

In the following sections we derive the field theory for the DTLAF close to $\chi = 1$ which describes the role played by the goldstone modes in determining the ground state. The TLAF end is already very well studied and our calculations in this end are done with a view of the TLAF as a reference point. Before presenting the calculations on the TLAF we briefly describe here the method of using the $SU(2)$ coherent state basis to derive the path integral representation of any spin system.

3.1 Lattice model to continuum Field Theory.

In order to go from the array of quantum spins to a semiclassical continuum field theory we need to make a suitable choice of basis to represent the spins. The spin coherent state basis forms a good representation that meets our needs [32]. In this section we describe this basis and the procedure by which to go from the microscopic lattice model to the continuum field theory. We first present for completeness a treatment given by Fradkin [33] and later adapt it to our specific model.

Firstly, the transformation from the basis in which $\mathbf{S}^2$ and S^z are diagonal, namely, $|S, M\rangle$ to the coherent state basis $|\hat{n}\rangle$ which are parametrised by the unit vector $\hat{n}$ is given by the following equation,

$$|\hat{n}\rangle = \sum_{-s}^{s} D^{(s)}(\hat{n})_{M,S} |S, M\rangle \tag{3.1}$$

Here, $\hat{n}$ takes values parametrised by points on S^2 the unit sphere and the unitary matrices $D^{(s)}(\hat{n})$ satisfy the relations,

$$D^{(s)}(\hat{n_1}) D^{(S)}(\hat{n_2}) = D^{(S)}(\hat{n_3}) \exp^{i\Phi(n_1,n_2,n_3)S_3} \tag{3.2}$$

Where, $\Phi(n_1, n_2, n_3)$ is the area of the spherical triangle drawn on the surface of the sphere S^2 and bounded by the points n_1, n_2, n_3. The different states $|n_i\rangle$ are not mutually orthogonal, but have a non-vanishing overlap given by

$$\langle n_1 | | n_2 \rangle = \exp^{i\Phi(n_1 n_2 n_0)} \left(\frac{1 + \hat{n_1}.\hat{n_2}}{2} \right)^S \tag{3.3}$$

and the resolution of identity which is written as follows makes it possible to use this set of (overcomplete) states as a continuous basis set to express the

spin operators.

$$\int d\mu(n) \, | \hat{n} \rangle \langle \hat{n} | = \mathbf{I} \tag{3.4}$$

where the measure is given by $d\mu(n) = \frac{2S+1}{4\pi} \; d^3n \;\; \delta(\vec{n}^2 - 1)$. The diagonal matrix elements of the spin operator $\vec{S}$ in this basis is given by,

$$\langle \hat{n} \, | \vec{S} \, | \hat{n} \rangle = S\hat{n} \tag{3.5}$$

The path integral for the evolution of one spin in time may be represented in this basis by dividing the time axis into intervals of length δt and sandwiching the identity operator of equation (3.4) at each point. Slicing up the partition function into N_t time intervals, we have,

$$\begin{aligned} Z &= \mathrm{Tr} \exp^{-\beta H} \\ &= \lim_{\{N_t, \delta_t\} \to \{\infty, 0\}} \left(\exp^{-\delta t H} \right)^{N_t} \end{aligned} \tag{3.6}$$

Now introducing the resolution of identity at every intermediate stage we get the required description of the path integral below,

$$Z = \lim_{\{N_t, \delta_t\} \to \{\infty, 0\}} \left[\prod_{j=1}^{N_t} \int d\mu(\vec{n_j}) \prod_{j=1}^{N_t} \langle n(t_j) \, | \exp^{-\delta t H} \, | n(t_j + 1) \rangle \right] \tag{3.7}$$

This can be rewritten as follows

$$Z = \lim_{\{N_t, \delta_t\} \to \{\infty, 0\}} \int D\vec{n} \exp^{-S(\vec{n})} \tag{3.8}$$

where $S(\vec{n})$ is given by the expression,

$$\begin{aligned} -S(\vec{n}) &= iS\sum_{j=1}^{N_t}\Phi(\vec{n_0},\vec{n_{t_j}},\vec{n_{t_{j+1}}}) + S\sum_{j=1}^{N_t}\log\left(\frac{1+\vec{n(t_j)}.\vec{n(t_{j+1})}}{2}\right) \\ &\quad -\sum_{j=1}^{N_t}\langle n(t_j)\,|\,H\,|\,n(t_{j+1})\rangle \end{aligned} \tag{3.9}$$

The first term $\Omega - iS\sum_{j=1}^{N_t}\Phi(\vec{n_0},\vec{n_{t_j}},\vec{n_{t_{j+1}}})$ is the solid angle subtended by the three vectors $\vec{n_i}$ which parametrise Φ at the centre of the sphere. This is the Berry's phase associated with the evolution of the spin in time over the time interval 0 to β which has been sliced up into intervals of duration δt. Ω is the sum of the contributions such as Φ of elementary areas bounded by the points $\{n_0, n_{t_j}, n_{t_{j+1}}\}$ on the surface of the parameter space defined by the sphere S^2 and can be written as follows,

$$\begin{aligned} \Omega &= \sum_{j=1}^{N_t}\Phi(\vec{n_0},\vec{n_{t_j}},\vec{n_{t_{j+1}}}) \\ &= \int_0^1 \mathrm{d}\tau\int_0^\beta \mathrm{dt}\;\; \vec{n(t,\tau)}.\partial_t\vec{n(t,\tau)}\times\partial_t\vec{n(t,\tau)} \end{aligned} \tag{3.10}$$

where, $n(t,\tau)$ is an arbitrary extension of n(t) from its value on the boundary, into the cap Σ which is bounded by n(t), subject to the conditions,

$$\vec{n}(t,0) = \vec{n}(t) \quad ; \quad \vec{n}(t,1) = \vec{n}_o \quad \text{and} \quad \vec{n}(0,\tau) = \vec{n}(\beta,\tau) \tag{3.11}$$

and t $\epsilon[0,\beta]$, $\tau\epsilon[0,1]$.

Before continuing to discuss equation (3.9) we switch to notations which will be used in the following sections to rewrite Ω in a different form. We rewrite Φ in terms of $\mathbf{n} = \vec{n}^a.\tau^a$ so that the solid angle term is rewritten as,

$$\Omega = \int_0^\beta\int_0^1 dtd\tau\frac{1}{2i}Tr\left[\mathbf{n}(t,\tau)\partial_t\mathbf{n}(t,\tau)\partial_\tau\mathbf{n}(t,\tau)\right] \tag{3.12}$$

The fluctuations of n about a classical value $\{\mathrm{n}_\alpha^{cl}\}$, can be expressed as,

$$\mathrm{n}(t,\tau) = U^\dagger(t,\tau)\mathrm{n}_\alpha^{cl}U(t,\tau) \tag{3.13}$$

Ω can be written in terms of the fields $l_\mu = i\partial_\mu UU^\dagger$ as follows

$$\Omega = \int_0^\beta \int_0^t dtd\tau Tr[\mathrm{n}_\alpha^{cl}(\partial_\tau l_t - \partial_t l_\tau)] \tag{3.14}$$

In the above expression, we separate out U(t,τ) as

$$U(t,\tau) = V(\tau)W(t) \tag{3.15}$$

which meet the conditions (3.11) so that, $\partial_t l_\tau = 0$, $\partial_\tau l_t = \partial_\tau(VL_tV^\dagger)$ where $L_t = i\partial_t WW^\dagger$ and substituting this expression in equation (3.14) we get,

$$\Omega = -i\int_0^\beta dtTr[W^\dagger \mathrm{n}_\alpha^{cl}\partial_t W] \tag{3.16}$$

To resume the exposition of the equation(3.9), the second term is seen to vanish in the limit of $\mathrm{N}_t \to \infty$ and $\delta t \to 0$ while the last term, in this limit reduces to the diagonal matrix element of the Hamiltonian $\langle n(t_j) \mid H \mid n(t_j)\rangle$.

This formalism is trivially extended to the case of a two dimensional spin array. In this case, the $\vec{n}$ now carry an index i which labels the lattice site. The berry phase terms simply add up as indicated by a sum over the index i, the hamiltonian for the single spin has to be replaced by the Hamiltonian for the interacting spin model. Having made these changes, the expression for the action is,

$$S(\vec{n}) = -iS\sum_i \Omega_i(\vec{n_i}) + \int_0^\beta \mathrm{dt} \sum_{<i,j>} JS^2\vec{n}_i(t).\vec{n}_j(t) \tag{3.17}$$

This is the basic procedure to construct a Euclidean path integral starting from a lattice spin system. It must be noted that this expression is still in terms of the Lattice model. Our aim will be to present a coarse grained picture in terms of slowly varying gapless modes of the theory which will be described in the next section.

3.2 Long Wavelength Low Energy Effective Action

In this section, we describe the procedure of obtaining the parameters of the effective field theory of the DTLAF near $\chi = 1$. In this section, we refer to the notation that has been established in chapter (2) with respect to labelling of lattice sites, the different low energy modes etc.

The modes which are relevant in this end, are the three gapless goldstone modes, the S-S modes, therefore the theory is designed to allow for large fluctuations in these modes, while the H-H and the H-S modes are integrated out in a quadratic approximation. In order to make a distinction between these different modes we rewrite the spins as follows,

$$\mathbf{S}_{Ii\alpha} = SW_I^{\dagger}\ \exp^{-\frac{w_{Ii\alpha}}{\sqrt{s}}}\ \mathbf{n}_{\alpha}\ \exp^{\frac{w_{Ii\alpha}}{\sqrt{s}}}\ W_I \tag{3.18}$$

In the above expression, the $\exp^{\frac{w_{Ii\alpha}}{\sqrt{s}}}$ contains the H-H and H-S modes and the W_I contains the S-S modes alone. The energy cost of exciting the modes parametrised by the $w_{Ii\alpha}$ are down by an order $\frac{1}{s}$ compared to the goldstone modes, therefore we retain only terms quadratic in the $w_{Ii\alpha}$ which will contribute to the effective action in this order.

We then make a gradient expansion of the fields W_I and retain out of this expansion, terms involving up to two spatial derivatives only since we are interested in the long wavelength limit.

The expression for the action at this stage contains terms that couple the hard and soft modes. Integrating out the hard modes constitutes the final stage in the construction of the effective action.

As described in the previous section, the action that we wish to estimate is given by,

$$S = \int d\tau \sum_{I i \alpha} \Omega_{I,i,\alpha} + \sum_{I i \alpha, J j \beta} \mathbf{H}_{I i \alpha, J j \beta} \tag{3.19}$$

where, $\Omega_{I i \alpha}$ is the total solid angle subtended by the evolution of each spin and this term is given in terms of the fields W by the following expression.

$$\Omega = i S U^{\dagger}_{I i \alpha} n_{\alpha} \partial_{\tau} U_{I i \alpha} \tag{3.20}$$

where, $U_{I i \alpha} = \exp^{\frac{w_{I i \alpha}}{\sqrt{i}}} W_I$, while the interaction part $\mathbf{H}$ is given by,

$$\mathbf{H}_{I i \alpha, J j \beta} = \frac{J S^2}{2} \sum_{< I i \alpha, J j \beta >} \mathrm{Tr}\left[\mathbf{n}_{I i \alpha} \mathbf{n}_{J j \beta}\right] \tag{3.21}$$

Before we make a long wavelength expansion, we regroup the different terms in the above expression and rewrite $\mathbf{H}$ as follows,

$$\mathbf{H}_{I i \alpha, J j \beta} = \frac{J S^2}{2} Tr \left\{ \mathbf{n}_{I i \alpha} \left[\mathbf{J}^0{}_{i \alpha j \beta}\, \delta_{I,J} + \frac{1}{2} \mathbf{J}^r{}_{i \alpha j \beta}\, \delta_{I+E_r,J} + \frac{1}{2} (\mathbf{J}^r{}_{i \alpha j \beta})^T \delta_{I-E_r,J} \right] \mathbf{n}_{J j \beta} \right\} \tag{3.22}$$

where, the matrices $\mathbf{J}^0$ count the bonds between spins in one unit cell and the matrices $\mathbf{J}^r$ count the bonds between spins on unit cells I and I + E_r, while

$(\mathbf{J}^{rT}{}_{i\alpha j\beta})$ count the bonds between spins on unit cells indexed by I and I - E_r, as indicated by the associated Kronecker delta. The explicit expressions for the matrices $\mathbf{J}$ are given in Appendix B.

The long wavelength expansion involves writing the associated Kronecker deltas as follows,

$$\delta_{I+E_r,J} = \delta_{I,J} \left[1 + \mathrm{E}_r^k \nabla_k + \frac{1}{2}\mathrm{E}_r^k \mathrm{E}_r^l \nabla_k \nabla_l\right] \tag{3.23}$$

where $\mathrm{E}_r^k \nabla_k = \partial_r$ in terms of which the equation (3.22) is given by,

$$\begin{aligned}\mathbf{H} = \frac{JS^2}{2} Tr \Big\{ \mathbf{n}_{Ii\alpha} \Big[& \mathbf{J}^0{}_{i\alpha j\beta} + \frac{1}{2}(\mathbf{J}^r{}_{i\alpha j\beta} + (\mathbf{J}^{rT}{}_{i\alpha j\beta})) \\ & - \frac{1}{2}(\mathbf{J}^r{}_{i\alpha j\beta} - (\mathbf{J}^{rT}{}_{i\alpha j\beta}))\partial_r \\ & + \frac{1}{4}(\mathbf{J}^r{}_{i\alpha j\beta} + (\mathbf{J}^{rT}{}_{i\alpha j\beta}))\partial_r^2 \Big] \mathbf{n}_{Ij\beta} \Big\}\end{aligned} \tag{3.24}$$

We now expand the $\mathbf{n}_{Ii\alpha}$ as in equation (3.18) where the spins $S_{Ii\alpha}$ are expressed in terms of the soft modes contained in W and the remaining degrees of freedom $w_{Ii\alpha}$ and evaluate equation (3.24) rewriting gradients of W in terms of the chiral fields $L_\mu = i\partial_\mu W W^\dagger$, which reads as follows.

$$\mathbf{H} = \mathbf{H}_{ww} + \mathbf{H}_{wL} + \mathbf{H}_{LL} \tag{3.25}$$

where $\mathbf{H}_{ww}$ contains the part which is purely in terms of the hard modes and is given by,

$$\mathbf{H}_{pp} + \mathbf{H}_{qq} = \sum_{nr} m_{nr}^{-1} P_{nr}^* P_{nr} + k_{nr} Q_{nr}^* Q_{nr} \tag{3.26}$$

as before and the $\mathbf{H}_{wL}$ contains the overlap between the hard and the soft modes given by,

$$\mathbf{H}_{qL} = JS\sqrt{S}[C_{nr}^1 P_{nr} + C_{nr}^2 Q_{nr} + h.c] \tag{3.27}$$

where C^{i}_{nr} are given in the appendix B. The last part is purely in terms of the soft modes and comes from the last term in equation 3.24. Performing the Gaussian integral over the hard degrees of freedom P and Q also gives terms that add to $\mathbf{H}_{LL}$.

To get the right expression for the Lagrangian density as we go from the Lattice to the continuum version, we have to divide by the volume of the Brillouin zone, which is equal to the integral over the density of states and is given by the equation,

$$\pi\Lambda^2 = \frac{2\pi^2}{3\sqrt{3}} \tag{3.28}$$

The final expression for S that we obtain after performing this integration involves only the S-S modes in the form of the matrix W but has parameters that have incorporated the effects of the other hard fluctuations. This form of the effective action reads as follows,

$$S = \int_{\Lambda} d^3x \frac{1}{2} \sum_{\substack{\mu=0,2 \\ a=1,3}} \rho^a_\mu L^a_\mu L^a_\mu \tag{3.29}$$

The suffix Λ indicates that the action is defined with an upper cut off on the wave vectors equal to Λ. This parameter is naturally imposed by the fact that we do not allow for fluctuations at length scales smaller than the unit cell.

Drawing on the analogy of the above action with that for coupled rigid bodies, $\rho^a_0 = I^a$ gives the moment of inertia for rotations about the axis X^a in spin space, and $\rho^a_i = \rho^a$ give the corresponding spin wave stiffnesses. In terms

of χ the I^a are,

$$\begin{aligned} I^3 &= \frac{1}{J}\frac{4}{9\sqrt{3}}\frac{(3-\chi)}{\chi(2-\chi)} \\ I^{1,2} &= \frac{1}{J}\frac{4}{9\sqrt{3}}\frac{(3+7\chi)}{\chi(4+\chi)} \end{aligned} \tag{3.30}$$

and the ρ^a are given by,

$$\begin{aligned} \rho^3 &= JS^2\sqrt{3}\,(1+\chi) \\ \rho^{1,2} &= JS^2\sqrt{3}\,\frac{\chi(5-\chi)}{(3+\chi)} \end{aligned} \tag{3.31}$$

At this point we match our results with the calculation of the parameters of the field theory describing the Triangular lattice by Dombre and Read [9]. In order to compare with their expressions for the TLAF, we evaluate equations (3.30 - 3.31) for the case $\chi = 1$. The action of Dombre and Read is given by the expression,

$$S = \int_\Lambda JS^2 \left\{ \frac{4}{9\sqrt{3}}\mathbf{L}_0^a\mathbf{L}_0^a + \frac{\sqrt{3}}{2}\mathbf{L}_i^3\mathbf{L}_i^3 + \sqrt{3}\mathbf{L}_i^j\mathbf{L}_i^j \right\} \tag{3.32}$$

Our values for the parameters I^a and ρ^a are as follows.

$$\begin{aligned} \rho^{1,2} &= JS^2\sqrt{3} \\ \rho^3 &= JS^2 2\sqrt{3} \\ I^{1,2,3} &= \frac{1}{J}\frac{4}{9\sqrt{3}} \end{aligned} \tag{3.33}$$

We find that when the action of Dombre and Read is written in terms of the fields L_μ^a the action has the form given above and the parameters ρ and I match well with the corresponding values from our derivation given here.

3.3 Symmetries of the effective action near $\chi = 1$

The original spin hamiltonian is invariant under the $SO(3)$ spin rotations. This corresponds to the spins $S_{Ii\alpha}$ transforming as follows,

$$S^a_{Ii\alpha} \rightarrow (\Omega_R)^a_b S^b_{Ii\alpha} \tag{3.34}$$

Where Ω_R is a $SO(3)$ matrix. In terms of the matrices $S_{Ii\alpha}$,

$$S_{Ii\alpha} \rightarrow X^\dagger S_{Ii\alpha} X \tag{3.35}$$

where X is the SU(2) representative of the matrix Ω_R. This corresponds to the transformation,

$$W(x) \rightarrow W(x)X \tag{3.36}$$

L_μ and hence the action in equation (3.29) is invariant under this transformation. We refer to this symmetry as the $SO(3)_R$ symmetry.

In addition the action is also invariant under the transformation ,

$$W(x) \rightarrow YW(x) \tag{3.37}$$

where $Y \in SO(2)$ and consists of matrices of the form $\exp i\theta\tau^3$. We refer to this symmetry as the $SO(2)_L$ symmetry. It acts on the spins as follows ,

$$S^a_{Ii\alpha} \rightarrow (\Omega_L)^\beta_\alpha S^a_{Ii\beta} \tag{3.38}$$

where Ω_L is the $SO(2)$ matrix corresponding to Y. This transformation is not a symmetry of the lattice model. It only arises in the continuum field theory [11]. This symmetry is observed in the lattice spin wave hamiltonian as a discrete Z_3 symmetry of rotation by 120° followed by translation by a unit lattice vector. The full internal symmetry group of the model is therefore $SO(3)_R \times SO(2)_L$.

3.4 Renormalization group analysis of the theory near $\chi = 1$

In this section, we describe a one loop renormalization group analysis of the $SO(3)_R \times SO(2)_L$ non-linear σ model described in equation (3.29). A model having this symmetry has been analyzed earlier by Azaria et al in [10]. We perform this calculation on our model with the parameters relating to the DT-LAF with a view to determining the phases described by it and the variation of the critical spin S_{cr}, the physical value of the spin above which the parameters lie in the ordered regime as a function of χ.

The action that we have derived in the previous section incorporates the effects of fluctuations at all length scales up to Λ_0, the cutoff wave vector. But we are interested in describing the physics of the system at $\mathbf{k} = 0$. In a perturbative calculation the higher $\mathbf{k}$ modes are directly integrated out at one step . The renormalization group program consists of integrating out the hard fluctuation modes shell by shell so that at each stage the effects of the faster $\mathbf{k}$ modes after being integrated out, serve to merely renormalize the coupling constants while giving an action having the same form as the bare action. This action is in terms of the softer modes only.

In the action S given in equation (3.29), which we address as S_{bare} in the following discussion the slow and fast degrees of freedom are separated by rewriting W as $\exp^{-i\pi}\tilde{W}$, where $\tilde{W}$ contains fluctuations with wave vectors ranging from $\mathbf{k} = 0$ to $\mathbf{k} = \Lambda_0 - \delta\Lambda = \Lambda_0 \exp^{-l}$. The π contain the fast fluctuations with $\mathbf{k}$ lying in the momentum shell $\Lambda_0 - \delta\Lambda$ to Λ_0.

With this separation of the fast and slow variables, equation (3.29) reads as

follows,

$$S_{bare} = S_1 + S_2 \tag{3.39}$$

$$S_1 = \int_{\Lambda_0-\delta\Lambda} d^3x \frac{1}{2} \sum_{\mu,a} \rho_\mu^a L_\mu^a L_\mu^a \tag{3.40}$$

$$S_2 = \int_{\Lambda_0-\delta\Lambda}^{\Lambda} d^3x \pi^a (D^{ab} + M^{ab}) \pi^b \tag{3.41}$$

where S_1 contains the fluctuations at all scales up to $\Lambda_0 - \delta\Lambda$ and S_2 contains those lying within the momentum shell Λ to $\Lambda_0 - \delta\Lambda$. The matrices D and M occurring in the expressions for S_2 are,

$$\begin{aligned} D^{ab} &= -\frac{1}{2}\delta^{ab}\left(\frac{\partial_0^2}{V_a^2} + \partial_i^2\right) = d_a \delta^{ab} \\ M^{ab} &= \epsilon^{abc} \frac{(\rho_\mu^c - (\rho_\mu^a + \rho_\mu^b))}{\rho^a} L_\mu^c \partial_\mu - 2\epsilon^{ack}\epsilon^{bdk} \frac{(\rho_\mu^d - \rho_\mu^k)}{\rho^a} L_\mu^c L_\mu^d \end{aligned} \tag{3.42}$$

Rescaling the measure such that the cutoff wavelength is once again Λ in equation (3.41), we get the effective action of the slower modes, as $S = S_{bare} + \delta S$. Here,

$$\delta S = \frac{\delta\Lambda}{\Lambda_0} S_{bare} - (1 + \frac{\delta\Lambda}{\Lambda_0}) \frac{1}{2} \int_{\Lambda_0-\delta\Lambda}^{\Lambda_0} \frac{d^3k}{(2\pi)^3} \langle k \,|\, \log(D + M) \,|\, k \rangle \tag{3.43}$$

Making use of the fact that log A may be written as $\log A = -\int_\epsilon^\infty \frac{ds}{s} \exp^{-sA}$, where $\epsilon = \frac{1}{\Lambda_0^2 c^2}$, we express δS as,

$$\delta S = \frac{\delta\Lambda}{\Lambda} S_{bare} \tag{3.44}$$

$$+ \frac{\delta\Lambda}{\Lambda} Tr \left[\sum_{a=1}^{3} (1 - \frac{M_{aa}}{\tilde{\Lambda}^2}) \exp - \frac{d_a}{2\tilde{\Lambda}^2} + \frac{(M_{12}M_{21})}{\tilde{\Lambda}^4} (\exp - \frac{d_1}{2\tilde{\Lambda}^2}) \right.$$

$$+\frac{2}{\tilde{\Lambda}^2}\left(\frac{M_{13}M_{31}+M_{23}M_{32}}{d_3-d_1}\right)\left(\exp-\frac{d_1}{2\tilde{\Lambda}^2}-\exp-\frac{d_3}{2\tilde{\Lambda}^2}\right)\Bigg]$$

The cutoff ϵ is meant to take care of the large k divergences. Evaluating these traces gives the final form for S in which the large momentum fluctuations in the shell $\Lambda_0 - \Lambda_0 \exp -l$ have been integrated out. The new S has the same form as the old one, the only change being that the coupling constants have been renormalized by the above operations. This process may be repeated shell by shell to obtain the low k action or equivalently solve the equations governing the flow of the coupling constants as larger length scales are approached. These R.G equations are written in terms of $g_a = \frac{1}{\sqrt{l_a \rho_a}}$ and $c_a = \sqrt{\frac{\rho_a}{l_a}}$. The equations governing the behaviour of the g_a are,

$$\begin{aligned}\frac{dg_1}{dl} &= -g_1+\lambda g_1^2\left(2-\frac{g_1}{g_3}\right)\\ \frac{dg_3}{dl} &= -g_3+\lambda\frac{g_1^2(c_1^2+c_3^2)}{2c_1c_3}\end{aligned} \tag{3.45}$$

The equations governing the flow of the c_a are,

$$\begin{aligned}\frac{dc_1}{dl} &= \lambda\,\frac{g_1^2c_1(c_3-c_1)}{g_3(c_3+c_1)}\\ \frac{dc_3}{dl} &= -\lambda\,\frac{g_1^2(c_3^2-c_1^2)}{2g_3c_1}\end{aligned} \tag{3.46}$$

Where $\lambda = \frac{\Lambda}{2\pi}$, in which the first term comes from naive scaling of the action and the second term is the one loop contribution coming from the trace.

We find however, by studying the behaviour of these equations for $c_1 - c_3 = \pm\nu$, for small values of ν, that they flow very quickly to $\nu = 0$ which for the two c_a equations is a fixed point. Therefore in the length scales that we are looking at, for all practical purposes we can set $c_1 = c_3$.

For $c_1 = c_3 = c$ the equations (3.45) reduce to,

$$\begin{aligned} \frac{dg_1}{dl} &= -g_1 + \frac{\Lambda g_1^2}{2\pi}(2 - \frac{g_1}{g_3}) \\ \frac{dg3}{dl} &= -g_3 + \frac{\Lambda g_1^2}{2\pi} \end{aligned} \tag{3.47}$$

We rescale the g_a such that $\bar{g}_a = \frac{\Lambda}{2} g_a$ and then substitute $\bar{g}_a = \gamma_a \exp^{-l}$. with this the above equations may be re-written as,

$$\begin{aligned} \frac{d\gamma_1}{dX} &= \gamma_1^2 \left(2 - \frac{\gamma_1}{\gamma_3}\right) \\ \frac{d\gamma_3}{dX} &= \gamma_1^2 \end{aligned} \tag{3.48}$$

with the variable l replaced by $X = 1 - \exp^{-l}$. These equations have the solution

$$\gamma_1 = \gamma_3 \pm \frac{a^2}{\gamma_3} \tag{3.49}$$

The critical line in the $g_1 - g_3$ plane is obtained by expressing the fact that the final values are asymptotically approached as X goes to 1. For example in equation 3.50, in which the equality defines for us the portion of the critical line for $\gamma_1 > \gamma_3$.

$$\int_{\gamma_3(0)}^{\infty} d\gamma_3 \, \frac{\gamma_3^2}{(\gamma_3^2 + a^2)^2} \leq 1 \tag{3.50}$$

Solving the conditions for small a yields the following expressions for the phase boundary, for $\gamma_1 > \gamma_3$,

$$\begin{aligned} \gamma_3 &= \frac{\pi}{4}t - \frac{t}{2}\tan^{-1}\ t + \frac{t}{4}\sin\left(2\tan^{-1}\ t\right) \\ \gamma_1 &= \gamma_3^0\left(\frac{1}{t^2}+1\right) \end{aligned}$$

where $t = \sqrt{\gamma_3^0/(\gamma_1^0 - \gamma_3^0)}$.

Similarly for $\gamma_1 < \gamma_3$

$$\begin{aligned} \gamma_3^0 &= \frac{1}{4t}\log\frac{1+t}{1-t} + \frac{1}{2(1-t^2)} \\ \gamma_1^0 &= \gamma_3^0(1-t^2) \end{aligned} \tag{3.51}$$

for $t = \sqrt{(\gamma_1^0 - \gamma_3^0)/\gamma_3^0}$.

For points lying on either sides of this critical surface, the equations have been solved numerically and fig 3.1 shows the flow diagram which indicates the way the coupling constants g_1 and g_3 evolve under renormalization.

In the figure the bare values at which we start off are indicated by crosses. For bare values g_0^a lying below the dashed curve the coupling constants flow to zero under this transformation. This is the renormalised classical phase in which the ground state possesses long range order and the classical expressions for the correlation lengths and coupling constants are merely renormalized by the quantum fluctuations.

For g_0^a lying above the curve, the parameters rapidly approach the Lorentz invariant $g_1 = g_2$ fixed point and for these values the system is quantum disordered.

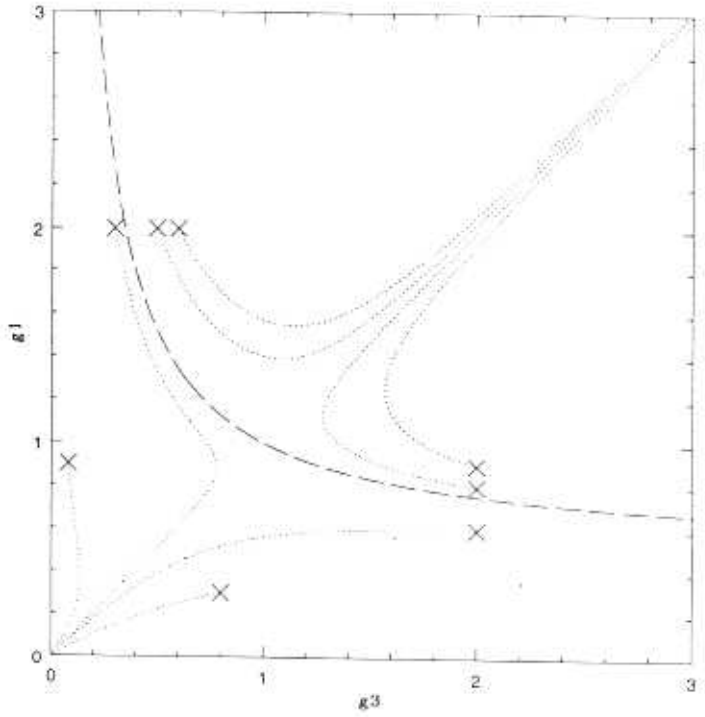

Figure 3.1: Flow diagram in the $g_1 - g_3$ plane, with flow lines starting from bare values indicated by crosses. The critical surface is represented by the dashed line.

In the context of the DTLAF, it is more illustrative to translate the description given here of the phase boundary into a relation between S_{crit} and χ. We find that for the entire range $0 \leq \chi \leq 2$ the values of g_1 is always greater than g_3. Therefore using the appropriate equations (3.51), we generate the curve of S_{crit} *vs* χ which is given in fig 3.2. In the figure we see that near $\chi = 1$ S_{crit} is almost constant and equal to 0.028 approximately. However this value is much smaller than we expect and the other effects could increase it sizeably. Secondly we see that S_{crit} decreases near $\chi = 0$. However the R.G equations that we derive do not hold good near this end as the field theory

itself does not take into account all the relevant modes near this end. Even

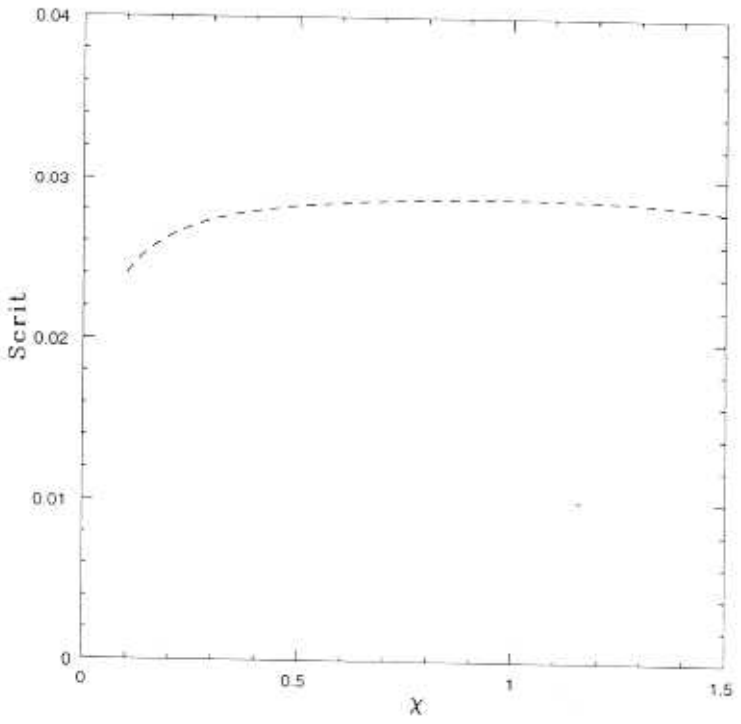

Figure 3.2: The dependence of S_{crit} on χ for the DTLAF in the range $0 < \chi < 1.5$.

qualitatively, we expect this picture to hold good only for models very close to the TLAF.

Lastly we have also checked if within the ordered phase, whether there exists a regime where g_1 and g_3 flow to zero with their ratios $\frac{g_1}{g_3}$ remaining finite. In such a regime the coupling constants would flow to values $\bar{g}_1, \bar{g}_3$ which could characterise a Nematic phase. This is because the stiffnesses being different for in plane and out of plane fluctuations, there would be a preferred planar configuration, which in turn has Nematic order. However there is no

such phase within this model.

Chapter 4

Phases in the DTLAF near $\chi = 0$

In this chapter, we propose a field theory to describe the DTLAF close to the $\chi = 0$ end and possibly including the KLAF. The relevant fields here are the Rotation matrices W and the unit vector field $\hat{m}$ which parametrise the S-S modes and the H-S modes respectively. This model has the same symmetries as the theory near $\chi = 1$ namely $SO(3)_R \times SO(2)_L$. In the weak coupling regime, when there is long range spin order the fields m^1 and m^2 have an equal and small gap. In the spin disordered regime, the fluctuations in W drive the system into a phase where the $SO(2)_L$ symmetry is broken and there is one gapless mode and one gapped mode. We present this as a mechanism that could be operative in the KLAF when approached through the $\sqrt{3} \times \sqrt{3}$ state. A suitable order parameter that characterizes this phase is the operator $\chi = \vec{S}_{j\nu}.\vec{S}_{i\alpha} \times \vec{S}_{i\beta}$.

4.1 Relevant fields near $\chi = 0$ and related symmetries

Referring to the classification of section (2.2) the relevant modes near the $\chi = 0$ end are the S-S and the H-S modes. In this section we describe one way to parametrise the 2 H-S modes Φ_{11} and Φ_{22} of section (2.4) in terms of quantities which are defined over each unit cell shown in figure 2.7, so that

field theory of the large amplitude long wavelength fluctuations of these modes can be written down. Such a parametrisation is achieved and the spins are written in terms of a unitary matrix W and a unit vector field $\hat{m}$.

Small fluctuations of the classical ground state configuration due to the H-S modes can be written using equation (2.13) as follows,

$$S_{Ii\alpha} = \tilde{s} n_\alpha + i\sqrt{\tilde{s}}[n_\alpha, w_{Ii\alpha}] \tag{4.1}$$

where, $w_{Ii\alpha}$ which contains only the H-S modes can be written as,

$$w_{Ii\alpha} i = [P^+ \Phi^{1,1}_{i\alpha} + P^- \Phi^{2,2}_{i\alpha}] \epsilon^1_\alpha \tag{4.2}$$

with $P^+ = (P^-)^* = P_1 - iP_2$.

We parametrise these modes for large amplitude fluctuations by rewriting the matrices $U_{Ii\alpha}$ in terms of the fields $\hat{m}_I$ as follows,

$$U_{Ii\alpha} = \exp i\frac{(i-1)\phi\tau^3}{2} \exp i\frac{\phi m_I}{4} \exp i\frac{(1-2i)\phi\tau^3}{4} \tag{4.3}$$

where $\phi = 2\pi/3$ and $m_I = \hat{m}_I.\vec{\tau}$. This expression reproduces equation(4.1) exactly when $\hat{m}$ is slightly deviating from $\hat{z}$. This can be seen by substituting $m_I = \tau^3 + \pi^1\tau^1 + \pi^2\tau^2$ and matching with equation (4.3) with the identification $\pi_1 = \frac{1}{3}P_2$ and $\pi_2 = \frac{1}{3}P_1$.

The complete expression for $U_{Ii\alpha}$ including the effects of the H-S, the H-H and the S-S modes can now be rewritten as,

$$U_{Ii\alpha} = \exp \frac{w_{Ii\alpha}}{\sqrt{\tilde{s}}} V_I W_I \tag{4.4}$$

where the $w_{Ii\alpha}$ is expanded in terms of the H-H modes alone, the V_I is given by the R.H.S of equation (4.3) and the SU(2) matrix W_I as earlier, contains

the S-S modes alone. As we can see from the expression (4.3) the amount by which the V_{Ii} deform each spin is dependent on the index i. Therefore this is a rotation which distorts the existing spin configuration within each unit cell. The W_I on the other hand cause a rotation of all spins within a unit cell without deforming their relative orientations.

We now examine the transformation properties of the new fields under the symmetries of the theory. First consider the $SO(3)_R$ spin rotation symmetry of the hamiltonian. The transformation of the spins as given in equation (3.35) is obtained if W transforms as given in equation (3.36) and if

$$m_I \rightarrow m_I \tag{4.5}$$

The $SO(2)_L$ symmetry, as mentioned in section (3.3) is not a symmetry of the spin system but is however a symmetry of the low energy, long wavelength field theory near $\lambda = 1$. We assume that this symmetry persists near $\lambda = 0$ also. Under the $SO(2)_L$ transformations the fields W transform as before, given by equations (3.37) and

$$m_I \rightarrow Y m_I Y^{\dagger} \tag{4.6}$$

Equations (3.36), (3.37), (4.5) and (4.6) then specify the transformation properties of the fields under the $SO(3)_R \times SO(2)_L$ symmetry of the low energy theory.

4.2 The Effective Field theory for small χ

We now motivate the form of the action that will effectively describe the phases of the DTLAF for small χ. We split up the action as,

$$S = S_m[m] + S_{int}[W, m] + S_W[W] \tag{4.7}$$

As stated above, we assume that the full symmetry of the model to be $SO(3)_R \times SO(2)_L$ in the continuum limit. Retaining terms quadratic in the derivatives, the most general form of S_m compatible with this is,

$$S_m = \int d^3x \frac{1}{g_2} \partial_\mu m^a \partial_\mu m^a + V(m^3) \tag{4.8}$$

This action is trivially invariant under the $SO(3)_R$ symmetry since $\hat{m}$ is a singlet under this symmetry. We have taken the derivative terms to have no XY asymmetry and instead to be symmetric under the full $SO(3)_L$ group as a simplifying assumption. From our earlier experience with the $\chi = 1$ field theory, we do not expect that this will make a qualitative change in the one-loop approximation we will be working with.

$V(m^3)$ however is symmetric only under $SO(2)_L$. At the classical level, a model defined by S_m has two phases. The disordered $SO(2)_L$ symmetric phase which occurs when $V(m^3)$ is minimised at $m^3 = \pm 1$ and the ordered $SO(2)_L$ broken phase when it is minimised at $m^3 \neq 1$. An explicit calculation of the effective potential by following the method outlined in chapter 3 gives the result,

$$V_{eff}(m^3) = \frac{27 J_1}{8} ((m^3)^2 - 1 - 4\chi)^2 \tag{4.9}$$

This potential shows a minimum at $m^3 = 1$. We therefore use the same form as above with general parameters λ_0 and η_0, with $\eta_0 = 1$ at the KLAF end.

$$V(m^3) = \frac{\lambda_0}{2}((m^3)^2 - \eta_0)^2 \tag{4.10}$$

Thus for $\eta_0 > 1$, we have the symmetric phase (classically), there are two modes with equal gaps which are equal to $\sqrt{g_2\lambda_0(\eta_0 - 1)}$. This was seen in the spin wave analysis itself. For $\eta_0 < 1$, the $SO(2)_I$ symmetry is broken. There is one gapless goldstone mode and the other mode has a gap.

The general form of S_W that retains terms quadratic in the derivatives and consistent with the symmetries of the theory is given by equation (3.29). To motivate the form of the interaction term, we note that the deviation of m^3 from ± 1 implies that the spin configuration is non-planar. To see this, we define vectors $\hat{C}_{Ii}$ as,

$$C_{Ii} = -\frac{2i}{3\sqrt{3}}\sum_{\alpha}[S_{Ii\alpha}, S_{Ii\alpha+1}] \tag{4.11}$$

where as usual $C_{Ii} = \hat{C}_{Ii}.\vec{\tau}$. $\hat{C}_{Ii}$ is the normal to the plane on which the 3 spins labelled by a particular value of i lie. Using equation (4.3) we have

$$C_{Ii} = e^{i\frac{(i-1)\phi\tau^3}{2}} e^{i\frac{\phi m_I}{2}} \tau^3 e^{-i\frac{\phi m_I}{2}} e^{-i\frac{(i-1)\phi\tau^3}{2}} \tag{4.12}$$

It is clear that when $\hat{m}$ deviates from $\hat{z}$, the vectors $\hat{C}_{Ii}$ are non- coplanar. It is known that non-planarity of the background spin configuration makes the gapless spin waves stiffer [13]. We therefore write down an interaction term of the form,

$$S_{int} = \int d^3x f(m^3) L^a_\mu L^a_\mu \tag{4.13}$$

INSTITUTE OF MATHEMATICAL SCIENCES

36821

Where $f(m^3)$ increases as $|m^3|$ decreases. One convenient choice for $f(m^3)$ is, $f(m^3) = -\alpha(m^3)^2$ with $\alpha > 0$.

In the next section, we analyse this theory with a view to seeing, in particular, if there is a phase in which the $SO(2)_L$ symmetry is broken and the $SO(3)_R$ spin symmetry is unbroken. As we saw in the previous chapters, at values of χ where the system is effectively described by a field theory of form given in equation (3.29), this does not happen. This is also described in detail in the references [34, 10, 11]. However, this does occur in the field theory given in equation (4.7) at the classical level if $\eta_0 < 1$. We have also argued that the unrenormalised value of η_0 is equal to 1. The potential $V(m^3)$ in equation (4.10) will get modified by the fluctuations of both the W and the $\vec{m}$ fields.

We now formulate a large N expansion to study the phases. We see that there are two phase transitions that take place. The first one takes the system from the spin ordered to the spin disordered $SO(2)_L$ symmetric phase. In the second transition, the fluctuations drive the model into a phase with the $SO(2)_L$ symmetry being broken.

4.3 Analysis of the $\chi = 0$ end of the DTLAF

In the following discussion we analyse the above theory in the strong coupling (large g_1 , g_3) regime where the W correlations are short ranged. In this regime, a renormalization group analysis which is an expansion in powers of the coupling constant is not applicable. One way of analysing this model in the strong coupling regime is through a $\frac{1}{N}$ expansion. We do this by enlarging

the $SO(3)_R$ symmetry of the theory to $SO(N)_R$ and then making a saddle point calculation which is valid in the large N limit.

4.3.1 The spin disordered phase by a large N expansion.

We begin by rewriting the fields W in terms of three unit vector fields ϕ_r^a which are given by the following relation,

$$\phi_r^a = \frac{1}{2} Tr[\tau^r W^\dagger \tau^a W] \tag{4.14}$$

In the following analysis we consider a corresponding theory in which the right index 'r' which varies from 1 to N , with the N component vectors ϕ_r^a satisfying the constraint

$$\sum_{r=1}^{N} \phi_r^a \phi_r^b = N[\frac{1}{\gamma_a} - \alpha(m^3)^2]\delta^{ab} \tag{4.15}$$

The interaction $\alpha(m^3)^2$ has been absorbed into the constraint equation. The γ_a are given in terms of the old coupling constants g_1 and g_3 by the expressions,

$$\frac{1}{\gamma_a} = 2(\frac{1}{g} - \frac{1}{g_a}) \quad ; \quad \frac{1}{g} = \frac{2}{g_1} + \frac{1}{g_3} \tag{4.16}$$

for a = 1,3.

We impose the above constraint on the ϕ fields by introducing some additional lagrange multiplier fields μ^{ab} and $\hat{m}$. This constraint is imposed by rewriting $\delta(\phi_r^a \phi_r^b - N(\frac{1}{\gamma_a}\delta^{ab} - \alpha m_3^2))$ in the following way,

$$\int D\mu \exp^{-\int d^d x i\mu^{ab}(\phi_r^a \phi_r^b - N(\frac{1}{\gamma_a}\delta^{ab}))} = \delta(\phi_r^a \phi_r^b - (N(\frac{1}{\gamma_a} - \alpha m_3^2)\delta^{ab})) \tag{4.17}$$

With these corrections the action that we wish to analyse reads as in equation (4.7), with $S_W + S_{int}$ being given by S_1,

$$S_1 = \int \sum_{a=1}^{N} \sum_{r=1}^{3} \partial_\mu \phi_r^a \partial_\mu \phi_r^a + i\mu^{ab}(\phi_r^a \phi_r^b - N(\frac{1}{\gamma_a} - \alpha(m^3)^2 \delta^{ab}) \tag{4.18}$$

$S_m = S_2$ is as given by equation (4.8), We scale the coupling constants g_2 and λ_0 by N so that this part of the action reads as follows,

$$S_2 = \int d^3x \frac{N}{g_2} \partial_\mu m^a \partial_\mu m^a + \frac{N\lambda_0}{2}((m^3)^2 - \eta_0)^2 \tag{4.19}$$

Where again the index a runs from 1 to 3. Integrating out the ϕ fields in this action, we get

$$S = \int d^3x \frac{N}{2} \mathrm{Tr} \log[-\partial_\mu^2 \delta^{ab} + i\mu^{ab}] - \frac{iN\mu^{aa}}{2}(\frac{1}{\gamma^a} - \alpha(m^3)^2)$$

$$+N \int d^3x \frac{1}{g_2} \partial_\mu m^a \partial_\mu m^a + \frac{\lambda_0}{2}((m^3)^2 - \eta_0)^2 \tag{4.20}$$

At the saddle point the action S is stationary about the field configurations. Therefore,

$$\frac{\delta S}{\delta \mu^{ab}} = 0 \tag{4.21}$$

$$\frac{\delta S}{\delta (m^3)^2} = 0 \tag{4.22}$$

Using these conditions, we get the following equations which are to be satisfied by the lagrange multiplier fields μ_{ab} and the fields $\hat{m}$. First, applying the condition (4.21) we get the following result,

$$(\frac{1}{\gamma_a} - \alpha(m^3)^2)(i\mu_{aa}) = \frac{1}{2} \int \frac{d^3k}{(2\pi)^3} [\frac{1}{K^2 + i\mu^2}(i\mu)]_{ab} \tag{4.23}$$

Applying the second condition (4.22) to the action we get,

$$2m^3\sqrt{1-(m^3)^2}(\lambda_0((m^3)^2-\eta_0)+i\alpha tr(\mu)=0 \tag{4.24}$$

Now putting in for $i\mu_{ab}$ the ansatz, $i\mu_{ab}=M_a^2\delta_{ab}$ we get,

$$\frac{1}{\gamma_a}-\alpha(m^3)^2=\frac{1}{2}\int\frac{d^3k}{(2\pi)^3}\frac{1}{K^2+M_a^2} \tag{4.25}$$

The other solution of the equations (4.21, 4.22) is $M_a=0$. Similiarly, for m^3 the solution is either

$$m_3^2=\eta_0-\frac{2\alpha M_a^2}{\lambda_0} \tag{4.26}$$

or it is $m^3=0$ or 1. By examining energies, it is easy to see that if a non-zero solution for M_a exists, then it is the minimum energy solution. Similiarly if $m^3\neq 1$ is a solution to equation (4.26) it minimizes the energy and otherwise the $m^3=1$ solution minimizes it. The solutions are obtained as follows.

A) If

$$\frac{1}{\gamma_a}-\alpha>\frac{1}{\gamma_{crit}} \tag{4.27}$$

where,

$$\frac{1}{\gamma_{crit}}=\int\frac{d^3K}{(2\pi)^3}\frac{1}{k^2}=\frac{\Lambda}{2\pi^2} \tag{4.28}$$

Then, $M_a=0$ and $m^3=1$ are the solutions. This describes an $SO(3)_R$ broken and $SO(2)_L$ symmetric phase. The low lying excitations are the three goldstone bosons.

B) When

$$\frac{1}{\gamma_a}-\alpha\leq\frac{1}{\gamma_{crit}} \tag{4.29}$$

Then $M_a \neq 0$ and $SO(3)_R$ is unbroken. In this disordered regime, the fields W have a finite correlation length which can be calculated by solving equation (4.25) to get M_a.

Further if

$$\eta_0 - \alpha M_a^2 \lambda_0 > 1 \tag{4.30}$$

Then $SO(2)_L$ is also unbroken.

C) The third possibility is when

$$\eta_0 - \alpha M_a^2 \lambda_0 > 1 \tag{4.31}$$

In this case, the $SO(2)_L$ symmetry is broken and the ϕ particle becomes massless. The field θ_m acquires a gap

Moving into the disordered regime is achieved in the DTLAF by reducing χ and thereby increasing g_a. Thus the above scenario can be translated into a phase diagram on the χ axis. For large $\chi \sim 1$ the ground state exhibits $\sqrt{3} \times \sqrt{3}$ order and the spin symmetry is broken. As χ is decreased to smaller values, the system disorders and we get into the second phase which is completely disordered. Further decreasing χ takes us into the $SO(2)_L$ broken phase.

We obtain the mass gap for the θ_m fluctuations which we will refer to in later sections. Rewriting the action S_m in terms of the variables θ_m and ϕ_m we get up to quadratic order in the fields,

$$S_m = \int d^3x \sin^2(\bar{\theta}_m)\partial_\mu\phi_m\partial_\mu\phi_m + \partial_\mu\theta_m\partial_\mu\theta_m + \frac{{M_\theta}^2}{2}(\theta_m)^2 \tag{4.32}$$

This mass gap can be calculated as follows, expanding S_m about the average value of $m_3 = \cos\bar{\theta}$ given in equation (4.26) we obtain the mass gap for excitations about $\bar{\theta}$ in 2 dimensions to be,

$$M_{\bar{\theta}}^2 = \frac{\lambda_0}{4g_2}\sin^2(2\bar{\theta}) \tag{4.33}$$

Substituting for $\bar{\theta}$ from equation (4.26) in the expression for $M_{\bar{\theta}}$ we get,

$$M_{\bar{\theta}}^2 = \frac{\lambda_0}{g_2}[\eta_0(1-\eta_0) - \frac{2\alpha M_a^2}{g_2}(1-2\eta_0)] \tag{4.34}$$

So far the discussion has been restricted to a regime where the $\hat{m}$ fields are approximated by their classical values.As we move into this $SO(2)_L$ ordered phase we must include the effects of fluctuations in the $\hat{m}$ and hence we still need to ascertain that including fluctuations in $\hat{m}$ does not destroy the order that has already been established.

4.3.2 Renormalization Group flows in the ordered phase.

Deep into the disordered phase the fluctuations of the Φ have a gap and can be integrated out. We will be left then with an action of the form of S_m in terms of $\hat{m}$ alone. Within this model we study the stability of the $SO(2)_L$ broken phase by a renormalization group analysis of S_m.

In this section, we investigate the effects of the $\hat{m}$ field fluctuations by a renormalization group analysis of S_m similar to our treatment of the $\lambda \sim 1$ theory. The one loop R.G equations can be computed using standard techniques.These equations simplify in terms of new variables, η' abd λ'. These

variables are, in terms of the old ones,

$$\lambda' = 2\lambda(\eta - 1) \tag{4.35}$$

$$\eta' = \frac{2\eta}{\eta + 1} \tag{4.36}$$

$$\tag{4.37}$$

The one loop renormalization group equations that govern their flow can be computed using standard techniques. These are as follows,

$$\frac{\partial g_2}{\partial l} = -g_2 + (g_2)^2 \tag{4.38}$$

$$\frac{\partial \lambda'}{\partial l} = 3\lambda(1 - g_2) \tag{4.39}$$

$$\frac{\partial \eta'}{\partial l} = 2g_2(\eta') \tag{4.40}$$

These equations can be explicitly solved to get,

$$g_2 = \frac{g_{20}\exp(-l)}{1 - g_{20}(1 - \exp(-l))} \tag{4.41}$$

$$\lambda' = \lambda'_0\,(1 - g_{20}(1 - \exp(-l)))^3\,\exp(3l) \tag{4.42}$$

$$\eta' = (\eta'_0)(1 - g_{20}(1 - \exp(-l)))^{-2} \tag{4.43}$$

When $g_{20} < g_{2crit} = 1$, g_2 flows to 0 and λ' flows to ∞. Therefore, in this range of g_{20}, The $SO(2)_L$ symmetry will be broken if $\eta(\infty) < 1$ and will be intact otherwise. This indicates that fluctuations tend to drive the system into disorder, however there exists a pocket in parameter space where the order is not destroyed completely. This is illustrated by the existence of a phase boundary separating the ordered and disordered phases. This phase boundary is obtained by setting $\eta'_\infty = 1$ in equation (4.43). This phase boundary is given by the equation,

$$\eta'_0 = (1 - g_{20})^2 \tag{4.44}$$

For parameters η_0' and g_{20} lying below this curve the system is in the ordered phase and otherwise it is in the disordered phase.

4.4 Correlation functions in the $SO(2)_L$ ordered phase.

In this section we describe the $SO(2)_L$ broken phase by defining a suitable order parameter in terms of the spins that acquires a long range order in this phase. In this phase the fields Φ are extremely short ranged since this is well into the $SO(3)_R$ broken regime. In computing the correlation functions there are therefore two types of averaging being done. First we average over the Φ fields and then over the fields θ_m and ϕ_m. For instance, consider the two point function of some local operator $\hat{O}(X)$ made out of the spins

$$G(X,Y) =< \hat{O}(X)\hat{O}(Y) > \tag{4.45}$$

This average involves an averaging over the Φ fields and the $\hat{m}$ fields. We denote that as follows.

$$G(X,Y) =<< O(X)O(Y) >_\Phi >_{\hat{m}} \tag{4.46}$$

If we are in the Φ disordered phase and look at $|X-Y| >> \xi_\Phi$, where ξ_Φ is the correlation length of the ϕ fields, then we have,

$$< \hat{O}(X)\hat{O}(Y) >_\Phi \sim < O(X)_\Phi >< O(Y)_\Phi > \tag{4.47}$$

At the mean field level in which we are working all the ϕ averages can be done using

$$\Phi_r^a(X)\Phi_s^b(X) = \frac{1}{\gamma_a}\delta^{ab}\delta_{rs} \tag{4.48}$$

Since we are in the SO(3) unbroken phase, the Φ average of any tensor operator has to be equal to a spin singlet multiplied by a constant tensor. (i.e a tensor made up of δ^{rs} and ϵ^{rsc}). Therefore we focus on operators which are scalar products or scalar triple products of spins.

We now analyse the behaviour of some singlet operators which could possibly characterise the $SO(2)_L$ symmetry broken phase. We consider operators of the form $\vec{S}_{i\alpha}.\vec{S}_{j\beta}$ and operators like $\vec{S}_{i\alpha}.\vec{S}_{j\beta} \times \vec{S}_{k\gamma}$ for various values of (i, α) etc. Taking account of the fact that the correlation of Φ^a_α are averaged as given above, we write down the expressions for the spin operator as,

$$\vec{S}_{i\alpha} = R^{-i+\frac{1}{2}} M R^{i-1} n_\alpha \tag{4.49}$$

where $n_{i+\alpha} = \exp(i\frac{2\pi}{3}T^3(i+\alpha))X$ Where in order to simplify calculations, the Φ are set to be equal to one and in the following discussion they are assumed to have been already integrated out. In the above expression, $R = \exp(\frac{2\pi i}{3}T^3)$ and $M = \exp(\frac{i\pi}{3}\hat{m}.\vec{T})$.

For any pair of spins $S_{i\alpha}$ and $S_{j\beta}$,

$$\vec{S}_{i\alpha}.\vec{S}_{j\beta} \;=\; n^T_\alpha R^{-i+1} M^T R^{i-j} M R^{j-1} n_\beta \tag{4.50}$$

In order to see the dependence of the above expression on θ_m and ϕ_m we rewrite $\hat{m}$ as,

$$\hat{m}.\vec{T} = \exp +i\phi T^3 \hat{m}_0.\vec{T} \exp -i\phi T^3 \tag{4.51}$$

We then have ,

$$\vec{S}_{i\alpha}.\vec{S}_{j\beta} = n^T_{i+\alpha-1+\phi} M_0^T R^{(i-j)} M_0 n_{\beta+j-1+\phi} \tag{4.52}$$

where we define,

$$M_0 = \exp^{\frac{i\pi}{3}\hat{m}_0.\vec{T}} \tag{4.53}$$

As ϕ_m is increased by π the above expression is invariant. This is a consequence of the vectors $n_{\alpha+\phi}$ being coplanar. This indicates that the dependence on ϕ_m is as $\exp(n\phi_M)$ where n = 0,2,4 ..

All such scalar products which we may define are not mutually independent. If referring to figure 2.7 we denote by T_1 the triangle with vertices (0,0), (1,1), (2,2). T_2 is the one with vertices (0,2), (1,0), (2,1), T_3 is made up of (0,1), (1,2), (2,0). Those products which are defined between pairs of spins from an up triangle T_1 in the unit cell is equivalent to that constructed from spins on the triangles T_2 and T_3. This is because of the property, $\vec{S}_{i+k,\alpha-k}.\vec{S}_{j+k,\beta-k} = \vec{S}_{i\alpha}.\vec{S}_{j\beta}$. Therefore for $i \neq j$, it is sufficient to compute among all the above pairs, those correlations that correspond to $A_i = \vec{S}_{ii}.\vec{S}_{i+1i+1}$ Also, for i = j the $\hat{m}$ dependences cancel to give, $\vec{S}_{i\alpha}.\vec{S}_{i\beta} = \hat{n}_\alpha.\hat{n}_\beta$

Among the scalar triple products, one simple operator which we evaluate here is

$$\chi_{ij} = \vec{S}_{j\gamma}.\vec{S}_{i\alpha} \times \vec{S}_{i\beta} \tag{4.54}$$

where, $\alpha \neq \beta \neq \gamma$ On substituting for the spins by the expression given in equation (4.49) this becomes,

$$\chi_{ij} = \frac{\sqrt{3}}{2} n^T_{\gamma+j-1} M^T R^{j-i} M Z \tag{4.55}$$

To obtain the actual expressions of these operators in terms of θ_m and ϕ_m it is necessary to find the elements of the matrix $\tilde{R} = M_0^T R M_0$. This matrix is

calculated and the entries are given in appendix C. We find that this has the form $\cos(\phi_1)F_1(\theta)+\sin(\phi_1)F_2(\theta)$ where $\phi_1 = (\gamma+j-1)\frac{2\pi}{3}+\phi_m$. Suitable linear combinations of these operators can be made which show a ϕ dependence of the form $\exp i\phi$. These operators $\exp(in\phi)$ form irreducible representations of the group $SO(2)_L$ and χij is the lowest in the hierarchy of such operators labelled by n. With reference to the figure of the unit cell(2.7) χ_{ij} when constructed out of three spins lying on a line such as (1,1), (0,0), (0,2) has the above form with n=1. For the set, (1,1),(1,2),(1,0) on the other hand n=0. From this dependence of χ on ϕ_m we expect that in the 2 -D classical limit, this operator will exhibit a power law decay of its correlation function below the Kosterlitz Thouless temperature.

4.4.1 Correlations of the Nematic order parameter.

We now make a comment on the behaviour of the order parameter N_{ab} studied by Chalker et al and Berlinsky et al [13, 23] which is defined as follows,

$$N_{ab}(x) = \frac{2}{3\sqrt{3}}[n_a^3(x)n_b^3(x) - \frac{1}{3}\delta_{ab}] \tag{4.56}$$

n^3 which is defined within a triangular plaquette is defined in equations (2.30). One important point is that N_{ab} differs from the spin 2 second rank nematic tensor which has been defined in equation (2.31) by the inclusion of singlet part $\bar{N}_{ab} = \frac{1}{3}\delta_{ab}(n_k^3 n_k^3 - 1)$ which spoils the transformation properties. This difference is important because of the following reason. When N_{ab} is defined on a planar spin configuration, the n^i can be normalised to have unit length at all points so that this difference vanishes. However when constructed out of

plaquette spins which are non-coplanar this cannot be done simultaneously at all points. When $\hat{m} \neq \hat{z}$, it creates non-coplanar configurations in which this part must be subtracted from the operator N_{ab} to get the right expression for Σ^{ab}

As mentioned in the introduction, one suggestion that has been put forth in order to understand the Kagome lattice problem is that it is a spin nematic. The suggestion is that the existence of gapless excitations in the Kagome lattice in the absence of long range spin order is due to long range order in the Nematic order parameter.

With the inclusion of the H-S modes non-planar configurations are excited in the KLAF and the nematic order parameter contains the scalar part described in the previous section. We first rewrite the nematic order parameter as follows,

$$\begin{aligned} N(x)_{ab}N(y)_{ba} &= \Sigma(x)_{ab}\Sigma(y)_{ab} \\ &+ \frac{4}{9\sqrt{3}}[1 - n_k^3(x)n_k^3(x)][1 - n_k^3(y)n_k^3(y)] \end{aligned} \tag{4.57}$$

In this, the first part being a spin two tensor, is short ranged in the $SO(3)_R$ broken phase and in the following section we evaluate the second part, which is the singlet part and find it to be dependent on θ_m.

$$< n^3.n^3 > \sim \sum_{i\alpha} \sum_{j\beta} S_{i\alpha} \times S_{i+1\alpha+1} . S_{j\beta} \times S_{j+1\beta+1} \tag{4.58}$$

The derivation of θ_m dependance of the correlations $< n^3.n^3 >$ is given in the appendix C.1. where we evaluate it for two different values of θ_m . Since

it turns out to be independent of ϕ_m it will be short ranged. However The θ_m dependence is strong.

$$< n^3.n^3 >= 1 + F(\theta) \neq const \tag{4.59}$$

As a consequence, in the $SO(2)_L$ broken phase we expect that the fields θ_m having a finite mass, will have short range correlations with a correlation length defined by M_θ. This will be however longer ranged than the spin spin correlations which are controlled by M_a. This is perhaps the reason that the spin spin correlations are found to decay much faster than the correlations of N_{ab}. Also the correlations fall off after some time saturating a constant.

Chapter 5

Summary and Conclusions.

5.1 Summary of the thesis

Apart from being an interesting model in itself, the DTLAF which has been described in chapter (2) provides a means of approaching the KLAF from the $\sqrt{3} \times \sqrt{3}$ ordered state. In this thesis, we propose and analyse a field theory that describes the long wavelength fluctuations about a $\sqrt{3} \times \sqrt{3}$ ordered state. This is related to a microscopic spin model on a KL with next nearest neighbour bonds which serve to stabilise this order.

In Chapter 2 we introduce the deformed triangular lattice antiferromagnet defined in equation (2.2) as a model which interpolates between the triangular and kagome lattices The classical ground state of this model throughout the range $0 < \chi \leq 1$, is independent of χ and is equal to the $\sqrt{3} \times \sqrt{3}$ state shown in figure (2.2). We perform a semiclassical, spin wave expansion about this classical ground state using the Holstein Primakoff formalism. This analysis tells us that the important low lying excitations are the gapless spin wave modes which we call the S-S modes. These are three in number and represent

rigid rotations of the spins in each unit cell. They correspond to the goldstone modes arising from the complete breaking of the SO(3) spin symmetry of the hamiltonian. Further there are two modes each with small and equal gaps which become gapless at $\chi = 0$. We address these modes as the H-S modes.

We calculate the individual contribution of these modes to the reduction of magnetization by means of a spin wave analysis. This indicates that the H-S modes are relevant not only for $\chi = 0$, the KLAF, but also for small non-zero values of χ. Figure 2.4 shows that this role of the H-S modes in reducing the local ordered moment becomes important below $\chi \sim 0.4$. The DTLAF therefore seems to undergo a phase transition near $\chi = 0.4$. The relevant modes for models with $\chi >> \chi_{crit} \sim 0.4$ are the three S-S modes and below χ_{crit} the relevant fields are the three S-S modes and the two H-S modes. Though the estimate of χ_{crit} may not be accurate, we expect that the small χ regime is a region that has a description different from the description of the phases above χ_{crit}.

We then approach the low χ regime through an alternate model which is the KLAF with next to nearest neighbour couplings. This is described by the hamiltonian of equation (2.40) which incorporates the effects of the weakening coupling χ in the DTLAF as $\chi = 0$ is approached. Using this model we obtain a parametrisation of the H-S modes for further study. From a calculation of the deformation produced in the spin configuration for small fluctuations we see that these modes generate non-planar configurations of spins.

We also calculate the reduction of other order parameters such as the Ne-

matic and staggered Chiral order parameters in the spin wave approximation. The chiral order parameter defined in equation (2.30) is sensitive to the chirality of the underlying spin configuration, whereas the Nematic operator is sensitive to the planarity of the same. In this approximation the reduction in the higher rank tensor operators such as the Chiral and Nematic order parameters, is found to be more that the reduction of the average staggered magnetization as we see in section (2.3).

In chapter 3 we describe in detail the derivation of the field theory of the S-S modes, which is a valid description of the DTLAF for $\chi > \chi_{crit}$. The theory is the $SO(3)_R \times SO(2)_L$ nonlinear sigma model, where $SO(3)_R$ is the spin symmetry of the hamiltonian and $SO(2)_L$ is an extra symmetry which is present in the low energy effective action. This arises from the three sublattice structure of the ground state about which this expansion is performed as discussed in section (3.3). The χ dependance of the parameters of this field theory is given in equations (3.30, 3.31). These equations are found to give results consistent with the earlier derivation by Dombre and Read for the triangular lattice.

We analyse this theory through a renormalization group method and obtain the flow diagram shown in figure 3.1 and dependance of the critical spin S_{crit} on χ. This tells us that the TLAF is well into the ordered phase even for the most quantum case of S= $\frac{1}{2}$. The actual value of S_{crit} obtained by this estimate is expected to be higher than our estimate which indicates that while giving a good qualitative picture, the parameters derived using this method are not very accurate.

We also investigate the possibility that the two coupling constants g_1 and g_3 will flow to zero with their ratio $\frac{g_1}{g_3} \neq 1$ thereby contributing differently toward the reduction in nematic and spiral order but we find that this does not happen for the derived range of parameters g_1 and g_3.

In chapter 4 we analyse the model in the small χ region, which is within the disordered regime of the W fields. Based on the results of spin wave analysis we propose a field theoretical model in section 4.2 that should adequately describe the KLAF and models in the DTLAF family close to it.

This action is in terms of the fields W and $\hat{m}$ which parametrise the S-S and H-S modes of section 2.2. The region that is of interest to us in this model is that for small χ. Namely into the phase where the fields W are disordered.

Probing the spin disordered phase by means of a large N mean field calculation gives interesting results. Initially within the strong coupling regime, the strong fluctuations in W drive the system into a phase where the spins are disordered. This phase has all the symmetries of the model intact. Further moving into the disordered phase shows that fluctuations tend to decrease the value of η and push the system into an $SO(2)_L$ broken phase (4.3.1). In this phase the symmetry between the two degrees of freedom labelled θ_m and ϕ_m is broken as the ϕ_m field fluctuations become massless and the θ_m are massive.

5.2 Conclusions

As mentioned in the introduction, one puzzle posed by experiments on the Kagome lattice compounds, Deuteronium Jarosite and $SrCr_8Ga_4O_{19}$ is that

there are massless low energy bosonic excitations as seen by the fact that the specific heat behaves as T^2. This is puzzling because there are no indications that the ground state has long range spin order taking into account the neutron scattering experiments, which indicate that there is very short ranged $\sqrt{3} \times \sqrt{3}$ order.

In the field theory we have proposed to describe the next nearest neighbour KLAF, we see interesting phases as we approach the KLAF end. In the regime close to the critical value of parameters, the correlation length for spin fluctuations is still large and in this phase all the symmetries of the model are intact. As we move more further into the disordered phase, or in this case, approach the KLAF, the $SO(2)_L$ symmetry breaks as described in the earlier chapter. In this phase, the polar variables θ_m and ϕ_m are the relevant variables. The fluctuations of the ϕ_m are the gapless spin 0 excitations. This is characterised by the appearance of long range order in the scalar operator χ_{ij} defined in equation (4.55). The existence of the massless excitation in the low energy spectrum of the KLAF could be due to the breaking of such a hidden $SO(2)_L$ symmetry in the low energy theory.

It is not possible to conclude definitely from our calculation if the lattice spin model actually works by this mechanism because the coupling constants of the field theory cannot be calculated meticulously. However evidence for gapless low lying excitations in a state without $\sqrt{3} \times \sqrt{3}$ order in the KLAF comes from an exact spectra analysis of the next to nearest neighbour KLAF model [35]. In this work, the authors give a plot of all the low lying levels in the spectrum which would collapse to the ground state as the number of

lattice sites $N \to \infty$. If the ground state should possess long range order those levels that collapse fastest to the ground state should form irreducible representations of the corresponding symmetry group, charactising that order.

In the TLAF, the nummber of lowest lying states is finite and this energy gap is found to increase linearly with S(S+1) thereby forming a pisa tower of states which is a signature of the symmetry broken ground state . On the contrary at the KLAF there is a rapid proliferation of low lying states which do not form this Pisa tower. This rapid proliferation of states and the absence of a tower of states with the gaps increasing linearly with $S(S+1)$ indicate that the $\sqrt{3} \times \sqrt{3}$ order is destroyed at the KLAF end.

In order to study the phase transition, they also plot the index R, which is an index of the fraction of those levels out of the set of all the low lying levels which are consistent with $\sqrt{3} \times \sqrt{3}$ order as a function of $\chi = J_2/J_1$. In order that the ground state should show $\sqrt{3} \times \sqrt{3}$ order, a large fraction of these states should have the matching symmetry. They see that while this index is 1 for the TLAF it drops abruptly to about 0.6 as χ is decreased indicating that at the corresponding value of $\chi = \chi_1$ the spins do disorder. What is of interest to us is that as χ is further decreased, there is another critical value of $\chi = \chi_2$ where again the index R jumps abruptly to zero indicating perhaps another phase transition.

This therefore is consistent with our picture of there being two phase transitions on approaching the KLAF from the TLAF end, through the $\sqrt{3} \times \sqrt{3}$ ordered state. A careful Monte Carlo simulation of the $J_1 - J_2$ KLAF, with a view

to observingthis phase transition would possibly verify our theory. Taking into account the different competing candidates groundstates of the KLAF, we feel that this approach to the KLAF starting from another groundstate, for instance the $\mathbf{q} = \mathbf{0}$ could also open up very interesting in this context.

Appendix A

Spin Wave Theory of the DTLAF

A.1 The matrices M^{-1} and K

$$
\begin{aligned}
M^{-1}_{i\alpha,j\beta} &= \frac{1}{2}[A_{i\alpha,j\beta} + 2(B^0 + B^1 + B^2)_{i\alpha,j\beta}] \\
K_{i\alpha,j\beta} &= \frac{1}{2}[A_{i\alpha,j\beta} \otimes I_{\alpha,\beta} - (B^0 + B^1 + B^2)_{i\alpha,j\beta}]
\end{aligned}
$$

The matrices A and $B^{0,1,2}$ can be written as $3 \times 3 \otimes 4 \times 4$ blocks as follows ,

$$
A = \begin{bmatrix} \tilde{A} & 0 & 0 \\ 0 & \tilde{A} & 0 \\ 0 & 0 & \tilde{A} \end{bmatrix} \qquad B_0 = \tfrac{1}{2} \begin{bmatrix} 0 & \tilde{B} & \tilde{B}^T \\ \tilde{B}^T & 0 & \tilde{B} \\ \tilde{B} & \tilde{B}^T & 0 \end{bmatrix}
$$

$$
B_1 + B_2 = \tfrac{1}{2} \begin{bmatrix} 0 & \tilde{B}_1 & \tilde{B}_2{}^\dagger \\ \tilde{B}_1{}^\dagger & 0 & \tilde{B}_3 \\ \tilde{B}_2 & \tilde{B}_3{}^\dagger & 0 \end{bmatrix}
$$

$$\tilde{A}_{i,j} = \begin{bmatrix} \chi+2 & 0 & 0 & 0 \\ 0 & \chi+2 & 0 & 0 \\ 0 & 0 & \chi+2 & 0 \\ 0 & 0 & 0 & 3\chi \end{bmatrix} \qquad \tilde{B}_{i,j} = \begin{bmatrix} 1 & 1 & 0 & \chi \\ 0 & 1 & 1 & \chi \\ 1 & 0 & 1 & \chi \\ \chi & \chi & \chi & 0 \end{bmatrix}$$

and

$$B_1 + B_2 = \tfrac{1}{2} \begin{bmatrix} 0 & \tilde{B}_1 & \tilde{B}_2{}^\dagger \\ \tilde{B}_1{}^\dagger & 0 & \tilde{B}_3 \\ \tilde{B}_2 & \tilde{B}_3{}^\dagger & 0 \end{bmatrix}$$

$$\tilde{B}_1(K) = \begin{bmatrix} 0 & 0 & 0 & \\ 0 & F(-K_2) & 0 & 0 \\ 0 & 0 & F(K_2) & \chi F(-K_3) \\ 0 & \chi F(K_1) & 0 & 0 \end{bmatrix}$$

$$\tilde{B}_2(K_1, K_2, K_3) = \tilde{B}_1(K_2, K_3, K_1) \tag{A.1}$$

$$\tilde{B}_3(K_1, K_2, K_3) = \tilde{B}_1(K_3, K_1, K_2) \tag{A.2}$$

where $F(K_i) = \exp^{iK_i} - 1$

A.2 The Eigenvectors of $\triangle\Omega^2$

$$\Phi^{nr}_{Li,\alpha} = \frac{1}{\sqrt{3}} L^{nr} \Psi^{nr}_{L,i} X^r_\alpha$$

$$\Phi^{nr}_{Ri,\alpha} = \frac{1}{\sqrt{3}} R^{nr} \Psi^{nr}_{R,i} X^r_\alpha$$

A.2.1 The vectors X^a

a	X^a
0	(1,1,1)
1	$(1, \alpha, \alpha^*)$
2	$(1, \alpha^*, \alpha)$

with the α being given by, $\alpha^3 = 1$

The following relations exist between the different $\Psi^{nr}_{L/R,i}$.

$$\Psi^{30}_R = \Psi^{*20}_R \quad \Psi^{30}_L = \Psi^{*20}_L$$

$$\Psi^{31}_R = \Psi^{*21}_R \quad \Psi^{31}_L = \Psi^{*21}_L$$

$$\Psi^{i2}_R = \Psi^{*i1}_R \quad \Psi^{i2}_L = \Psi^{*i1}_L$$

Therefore we tabulate here only the necessary and independant eigenvectors.

A.2.2 The vectors Ψ_R and Ψ_L

(n,r)	R^{nr} L^{nr}	Ψ_R^{nr} Ψ_L^{nr}
(0,0)	$\frac{1}{3-\chi}$ $\frac{1}{2}$	$(\chi, \chi, \chi, 6-5\chi)$ $(1,1,1,1)$
(1,0)	$\frac{1}{2\sqrt{3}}$ $\frac{1}{\sqrt{3}(3-\chi)}$	$(-1,-1,-1,3)$ $(5\chi-6, 5\chi-6, 5\chi-6, 3\chi)$
(2,0)	$\frac{1}{\sqrt{3}}$ $\frac{1}{\sqrt{3}}$	$(1, \alpha, \alpha^2, 0)$ $(1, \alpha, \alpha^2, 0)$
(0,1)	$\frac{1}{2}$ $\frac{1}{(7\chi+3)}$	$(1, 1, 1, 1)$ $(5\chi, 5\chi, 5\chi, (6-\chi))$
(1,1)	$\frac{1}{\sqrt{3}(3+7\chi)}$ $\frac{1}{2\sqrt{3}}$	$(\chi-6, \chi-6\chi-6, 15\chi)$ $(-1\ -1\ -1\ 3)$
(2,1)	$\frac{1}{\sqrt{3}}$ $\frac{1}{\sqrt{3}}$	$(1, \alpha, \alpha^2, 0)$ $(1, \alpha, \alpha^2, 0)$

A.3 The eigenvalues of $\triangle\Omega^2, \omega^2_{n,r}, c_{n,r}, c'_{n,r}$

(n,r)	$c_{n,r}$	$c'_{n,r}$	$\omega^2_{n,r}$
(0,0)	$\frac{9\chi(2-\chi)}{3-\chi}$	0	0
(1,0)	$\frac{3-\chi}{4}$	2χ	$\frac{\chi(3-\chi)}{2}$
(2,0)	$\frac{3+\chi}{2}$	$\frac{3+2\chi}{4}$	$\frac{(3+\chi)(2\chi+3)}{8}$
(3,0)	$\frac{3+\chi}{2}$	$\frac{3+2\chi}{4}$	$\frac{(3+\chi)(2\chi+3)}{8}$
(0,1)	0	$\frac{9\chi(4+\chi)}{2(7\chi+3)}$	0
(1,1)	2χ	$\frac{\chi(3+7\chi)}{4}$	$\frac{\chi(3+7\chi)}{4}$
(2,1)	$\frac{\chi+3}{2}$	$\frac{\chi+\frac{3}{2}}{2}$	$\frac{(\chi+3)(2\chi+3)}{8}$
(3,1)	$\frac{\chi}{2}$	$\frac{(\chi+3)}{2}$	$\frac{\chi(\chi+3)}{4}$
(0,2)	0	$\frac{9\chi(4+\chi)}{2(7\chi+3)}$	0
(1,2)	2χ	$\frac{(3+7\chi)}{8}$	$\frac{\chi(3+7\chi)}{4}$
(2,2)	$\frac{\chi+3}{2}$	$\frac{\chi+\frac{3}{2}}{2}$	$\frac{(\chi+3)(2\chi+3)}{8}$
(3,2)	$\frac{\chi}{2}$	$\frac{(\chi+3)}{2}$	$\frac{\chi(\chi+3)}{4}$

Appendix B

Integration of the Hard modes to get the effective Lagrangian

The calculation of the effective action involves integration of the hard modes which is described here. Using the notation of Chapter 3.2

$$\begin{aligned} \mathbf{H} &= \mathbf{H}_{ww} + \mathbf{H}_{wL} + \mathbf{H}_{LL} \\ \mathbf{H}_{ww} &= \mathbf{H}_{pp} + \mathbf{H}_{qq} \\ \mathbf{H}_{wL} &= \mathbf{H}_{qL} + \mathbf{H}_{pL} \end{aligned} \tag{B.1}$$

In the following text, we give the explicit forms of the above matrices. The matrix $\mathbf{H}_{ww}$ is given by the expression,

$$H_{pp} + H_{qq} = \sum P^{*}_{nr} P_{nr} m^{-1}_{nr} + Q^{*}_{nr} Q_{nr} k_{nr} \tag{B.2}$$

Where the factors M_{nr}^{-1} and k_{nr} are given by,

(n,r)	m_{nr}^{-1}	k_{nr}	(n,r)	m_{nr}^{-1}	k_{nr}
(1,1)	$\frac{9\chi(2-\chi}{6-2\chi}$	0	(1,2)	$\chi(6+14\chi)$	$\frac{9\chi(\chi+4)}{2(6+14\chi)}$
(1,3)	0	$\frac{9\chi(\chi+4)}{2(6+14\chi)}$	(2,1)	1	$2\chi(3-\chi)$
(2,2)	$\chi(6+14\chi)$	1/2	(2,3)	$\chi(6+14\chi)$	1/2
(3,1)	$(\chi+3)$	$\frac{2\chi+3}{2}$	(3,2)	$(\chi+3)$	$\frac{2\chi+3}{2}$
(3,3)	$(\chi+3)$	$\frac{2\chi+3}{2}$	(4,1)	$(\chi+3)$	$\frac{2\chi+3}{2}$
(4,2)	χ	$(\chi+3)$	(4,3)	χ	$(\chi+3)$

$$
\begin{aligned}
H_{ql} &= \sum_{nr} C_{nr}^2 Q_{nr} \\
&= -JS\sqrt{S}\ \{\ \frac{9\chi(4+\chi)}{3+7\chi}[q_{01}(L_1^3+iL_2^3)+q_{01}^*(L_1^3-iL_2^*)] \\
&\quad +\frac{5\sqrt{6}}{\sqrt{3+7\chi}}[q_{11}(L_1^3+iL_2^3)+q_{11}^*(L_1^3-iL_2^3)] \\
&\quad -2\sqrt{3}(2\chi+3)[q_{21}\alpha^*(L_1^3+iL_2^3)+q_{21}^*\alpha(L_1^3-iL_2^3)] \\
&\quad +2\sqrt{3}(\chi+3)[q_{31}\alpha(L_1^3+iL_2^3)+q_{31}^*\alpha^*(L_1^3-iL_2^3)]\}
\end{aligned}
\tag{B.3}
$$

$$
\text{and } H_{pL} = \sum_{n,r} C_{nr}^1 P_{nr} \tag{B.4}
$$

The C_{nr} can be simply tabulated as follows,

(n,r)	C^1_{nr}
(0,0)	$-\frac{2\chi(6-3\chi)}{\sqrt{3}(6-2\chi)} \quad L^k_\beta \epsilon^k_\beta$
(1,0)	$-\frac{2\chi}{\sqrt{3}\sqrt{18-6\chi}} \quad L^k_\beta \epsilon^k_\beta$
(2,0)	$\frac{2\chi\alpha^*}{3} \quad [L^k_\beta \epsilon^k_\beta + 2i\alpha^* \quad L^k_\beta n^k_\beta]$
(3,0)	$\frac{2\chi\alpha}{3} \quad [L^k_\beta \epsilon^k_\beta - 2i\alpha \quad L^k_\beta n^k_\beta \,]$
(1,1)	$-\frac{\chi\sqrt{6+14\chi}}{3} \quad [L^k_1 \epsilon^k_1 + L^k_2 \epsilon^k_2 + L^k_3 \epsilon^k_3]$
(2,1)	$-\frac{(6+4\chi)\alpha^*}{3} \quad [(L^k_1 \epsilon^k_1 + \alpha L^k_2 \epsilon^k_2 + \alpha^* L^k_3 \epsilon^k_3)$ $+ 6i(L^k_1 n^k_1 + \alpha L^k_2 n^k_2 + \alpha^* L^k_3 n^k_3)]$
(3,1)	$\frac{\alpha(6+2\chi)}{3} \quad [(L^k_1 \epsilon^k_1 + \alpha L^k_2 \epsilon^k_2 + \alpha^* + L^k_3 \epsilon^k_3)$ $- 6i(L^k_1 n^k_1 + \alpha L^k_2 n^k_2 + \alpha^* L^k_3 n^k_3) \,]$

The final action after performing this quadratic integration of the hard modes and the momenta conjugate to the soft modes is given in chapter 3.2

Appendix C

Form of the Correlation functions

First we write down the elements of the matrices A,B,C from sectionsecnematic. To begin with, the matrices $\tilde{R}$ are given by,

$$\tilde{R} = M_0^T R M_0 \tag{C.1}$$

and the entries $\tilde{R}_{ab}$ are given by,

$$\begin{aligned}
\tilde{R}_{11} &= -\frac{1}{2} + \frac{3}{8}\sin^2\theta_m \cos^2\theta_m \\
\tilde{R}_{22} &= -\frac{1}{2} + \frac{9}{8}\sin^2\theta_m \\
\tilde{R}_{12} &= -\frac{3\sqrt{3}}{8}\sin^2\theta_m \cos^2\theta_m - \sqrt{3}4(1+\cos^2\theta_m) \\
\tilde{R}_{21} &= -\frac{3\sqrt{3}}{8}\sin^2\theta_m \cos^2\theta_m + \sqrt{3}4(1+\cos^2\theta_m)
\end{aligned} \tag{C.2}$$

C.1 Correlations of the operator $n^3.n^3$

For the Triangle T_1 after shuffling the indices a bit the above terms can be rewritten as follows,

$$< n^3.n^3 > \;=\; (S_{ii}.S_{jj})(S_{i+1i+1}.S_{j+1j+1}) - (S_{ii}.S_{jj})(S_{i+1i+1}.S_{j-1j-1}) \tag{C.3}$$

When the spins are expressed as functions of θ_m and ϕ_m $\bar{N}_{ab}$ becomes,

$$\begin{aligned} < n^3.n^3 > &= 3 + (A + B + C)^2 \\ &\quad -2(A + B + C) - 2(A^2 + B^2 + C^2) \end{aligned} \tag{C.4}$$

Where, $A = \vec{S}_{00}.\vec{S}_{11}, B = \vec{S}_{11}.\vec{S}_{22}, C = \vec{S}_{22}.\vec{S}_{33}$

Putting in the expression for the $S_{i\alpha}$ in A , B , C, we get the following expressions,

$$A = n_2^T M^T R M R M R^T n_2 \tag{C.5}$$

$$B = n_1^T M^T R M R^T n_1 \tag{C.6}$$

$$C = n_0^T M^T R M R^T n_0 \tag{C.7}$$

In order to calculate A, B and C we need to calculate the elements,

With the understanding that $\phi_1 = (2i + 1)120°$ and $\phi_2 = (2i)120°$ we have,

$$\begin{aligned} n_{\phi_1}^T \tilde{R} n_{\phi_2} &= \rho_1 \cos(\phi_1 + \phi_2) + \rho_2 \sin(\phi_1 + \phi_2) \\ &\quad +\rho_3 \cos(\phi_1 - \phi_2) + \rho_4 \sin(\phi_1 - \phi_2) \end{aligned} \tag{C.8}$$

where,

$$\begin{aligned} \rho_1 &= \frac{3}{16} \sin^2\theta_m \cos^2\theta_m - \frac{9}{16} \sin^2\theta_m \\ \rho_2 &= -\frac{3\sqrt{3}}{8} \sin^2\theta_m \cos^2\theta_m \\ \rho_3 &= -\frac{1}{2} + \frac{3}{16} \sin^2\theta_m \cos^2\theta_m + \frac{9}{16} \sin^2\theta_m \\ \rho_4 &= \frac{\sqrt{3}}{4}(1 + \cos^2\theta_m) \end{aligned} \tag{C.9}$$

For $\theta_m = 0$ (or 1 respectively) the values of $\rho_1 - \rho_4$ are,

	$\theta_m = 0$	$\theta_{=\frac{\pi}{2}}$
ρ_1	0	$-\frac{9}{16}$
ρ_2	0	0
ρ_3	$-\frac{1}{2}$	$\frac{1}{16}$
ρ_4	$\frac{\sqrt{3}}{2}$	$\frac{\sqrt{3}}{2}$

The exact form of this function may be written down, but all we need to know to know is how it varies with ϕ_m and θ_m. That it is independant of ϕ_m is clear.

Substituting for ρ_a in the expressions for A,B,C and substituting in equation (C.4) to get the value of $< n^3.n^3 >$ we see thatitis not a constant function and is of the form $(1 + F(\theta_m))$.

Bibliography

[1] P.W.Anderson. *Phys.Rev.B*, 86, 1952.

[2] T. Jolicoeur and J.C. Le Guillou. *Phys.Rev.B*, 40:2727, 1989.

[3] P.W.Anderson. . *Science*, 235:1196, 1987.

[4] D.A. Huse and V. Elser. *Phys.Rev.Lett.*, 60:2531, 1988.

[5] N. Elstner, R.R.P. Singh and A.P. Young. *Phys.Rev.Lett*, 71:1629, 1993.

[6] B. Bernu, P. Lecheminant and C. L'huillier. . *Phys.Rev.B*, 50:10048, 1994.

[7] S. Chakravarty, B.I. Halperin and D.R. Nelson. *Phys.Rev.Lett.*, 60:1057, 1988.

[8] S. Chakravarty, B.I. Halperin and D.R. Nelson. *Phys.Rev.B.*, 39:2344, 1989.

[9] T. Dombre and N. Read. *Phys.Rev.B*, 39:6797, 1989.

[10] P. Azaria, B. Delamotte and D. Mouhanna. *Phys.Rev.Lett.*, 68:1762, 1992.

[11] P. Azaria, B. Delamotte, F. Deldue and T. Jolicoeur. *Nuc.Phys. B*, 485, 1993.

[12] P.Chandra, P.Coleman and I.Ritchey. . *Jour.Phys. Fr*, 3:591, 1993.

[13] Phys.Rev.Lett. J.T. Chalker, P.C.W. Holdsworth and E.F. Shender. *Phys.Rev.Lett*, 68:855, 1992.

[14] P. Chandra and P. Coleman. *Phys.Rev.Lett*, 66:100, 1991.

[15] P.Chandra, P.Coleman and A.I.Larkin. . *Jour.Phys. C*, 2:7933, 1990.

[16] X. Obradors, A. Labarta, A. Isalgue, J. Tejada, J. Rodriguez and M. Perret. *Sol.St.Comm*, 65:189, 1988.

[17] A.P. Ramirez, G.P. Espinosa and A.S. Cooper. *Phys.Rev.Lett.*, 64:2070, 1990.

[18] A.P. Ramirez, G.P. Espinosa and A.S. Cooper. *Phys.Rev.B*, 45:2505, 1992.

[19] C. Broholm, G. Aeppli, G.P. Espinosa and A.S. Cooper. *Phys.Rev.Lett*, 65:3173, 1990.

[20] A.S. Wills, A. Harrison, S.A.M. Mentink, T.E. Mason and Z. Tun. Magnetic correlations in deuteronium jarosite, a model $s = \frac{5}{2}$ kagome antiferromagnet. *cond-mat/9607106*, 1996.

[21] S.H.Lee, C.Broholm, M.F.Collins, L.Heller, A.P.Ramirez , C.Kloc, E.Bucher,R.W.Ervin and N.Lacevic. Less than 50 % sublattice polarization in an insulating S=3/2 kagome antiferromagnet at low T. *cond-mat/9705014*, :, 1997.

[22] M.G.Townsend, G.Longworth, E.Roudaut. . *Phys. Rev. B*, 33:4919, 1986.

[23] J.N. Reimers and A.J. Berlinsky Phys.Rev. *Phys.Rev.B*, 48:9539, 1993.

[24] Harris, C. Kallin and A.J. Berlinsky. *Phys.Rev.B*, 45:2899, 1992.

[25] A.Chubukov. *Phys.Rev.Lett*, 69:832, 1992.

[26] C. Zeng and V. Elser. *Phys.Rev.B*, 42:8436, 1990.

[27] J.T. Chalker and J.F.G. Eastmond. *Phys.Rev.B*, 46:14201, 1992.

[28] P.W.Leung and V.Elser. *Phys.Rev.B*, 47:5459, 1993.

[29] Rajiv.R.P. Singh and D.A. Huse. *Phys.Rev.Lett*, 68:1766, 1992.

[30] S.Sachdev. *Phys.Rev.B*, 45:12377, 1992.

[31] J.B. Marston and C. Zeng. *Jour.Appl.Phys.*, 69:5962, 1991.

[32] A.Perelomov. *Generalised Coherent States and their applications.* , .

[33] Eduardo. Fradkin. *Field Theories of Condensed Matter Systems.* Addison-Wesley,1991, Redwood City.

[34] D.H.Friedan. *Annals of Physics*, 163:318, 1985.

[35] P.Lecheminant, B.Bernu, C.L'huillier, L.Pierre and P.Sindzingre. Order versus disorder in the quantum heisenberg antiferromagnet on the kagome lattice: an approach through exact spectra analysis. *Phys.Rev.B*, 56:2521,2529, 1997.